

ARBITRARY LAGRANGIAN–EULERIAN DISCONTINUOUS GALERKIN METHOD FOR HYPERBOLIC EQUATIONS INVOLVING δ -SINGULARITIES*

XUE HONG[†] AND YINHUA XIA[†]

Abstract. In this paper, we develop and analyze an arbitrary Lagrangian–Eulerian discontinuous Galerkin (ALE-DG) method for solving one-dimensional hyperbolic equations involving δ -singularities on moving meshes. The L^2 and negative norm error estimates are proven for the ALE-DG approximation. More precisely, when choosing the approximation space with piecewise k th degree polynomials, the convergence rate in L^2 -norm for the scheme with the upwind numerical flux is $(k+1)$ th order in the region apart from the singularities, the convergence rate in $H^{-(k+1)}$ norm for the scheme with the monotone fluxes in the whole domain is k th order, the convergence rate in $H^{-(k+2)}$ norm for the scheme with the upwind flux in the whole domain can achieve $(k+\frac{1}{2})$ th order, and the convergence rate in $H^{-(k+1)}(R \setminus R_T)$ norm for the scheme with the upwind flux is $(2k+1)$ th order, where R_T is the pollution region at time T due to the singularities. Moreover, numerically the $(2k+1)$ th order accuracy for the postprocessed solution in the smooth region can be obtained, which is produced by convolving the ALE-DG solution with a suitable kernel consisting of B-splines. Numerical examples are shown to demonstrate the accuracy and capability of the ALE-DG method for the hyperbolic equations involving δ -singularity on moving meshes.

Key words. arbitrary Lagrangian–Eulerian discontinuous Galerkin method, hyperbolic equations, δ -singularities, moving meshes, error estimates

AMS subject classifications. 65M60, 35L67

DOI. 10.1137/19M1268008

1. Introduction. We are concerned with solving the following one-dimensional conservation laws involving δ -singularities:

$$(1.1) \quad \begin{cases} u_t + f(u)_x = h(x, t), & (x, t) \in \Omega \times (0, T], \\ u(x, 0) = u_0(x), & x \in \Omega, \end{cases}$$

where the source term $h(x, t)$, the initial condition $u_0(x)$, or the solution $u(x, t)$ may contain δ -singularities. A major challenge is how to capture these singularities and maintain the high resolution in the smooth region. Following the work of the DG method on static meshes [34] for this problem, we are interested in the arbitrary Lagrangian–Eulerian discontinuous Galerkin (ALE-DG) method on moving meshes. It has been demonstrated that the discontinuous Galerkin (DG) method based on the weak formulation can be applied directly to solve such problems without modifications and not severely smearing the singularities compared with other approximate methods [34]. The ALE-DG method considered in this paper provides an even smaller pollution region and thus better resolution in the smooth region. The rigorous error estimates for the DG method on static meshes were given in [34]. Similarly, L^2 and negative norm error estimates for the ALE-DG method can also be provided for the model problems involving δ -singularities.

*Received by the editors June 12, 2019; accepted for publication (in revised form) October 14, 2019; published electronically January 8, 2020.

<https://doi.org/10.1137/19M1268008>

Funding: The work of the second author was supported by the National Natural Science Foundation of China grant 11871449 and the Laboratory of Computational Physics grant 6142A0502020817.

[†]School of Mathematical Sciences, University of Science and Technology of China, Hefei, Anhui 230026, People's Republic of China (xuehong1@mail.ustc.edu.cn, yhxia@ustc.edu.cn).

The DG method is a class of finite element methods, in which the approximation space contains completely discontinuous, piecewise polynomials or other basis functions. The first DG scheme was constructed in 1973 by Reed and Hill [28] for the neutron transport equation, which is linear and time independent. Subsequently, Cockburn and co-authors developed the Runge–Kutta discontinuous Galerkin (RKDG) method for the nonlinear hyperbolic conservation laws in [10, 5, 7, 9] and also proved its high order accuracy in [8, 4]. Owing to the completely discontinuous approximation space, the DG method has some advantages like parallelization capability, shock capturing, high order accuracy, and so on. The DG method has a wide range of applications, and we refer to [6, 11, 12, 19, 33, 30] and the references therein for more references of the DG method.

The ALE-DG method discussed here is a moving mesh DG method and the grid moving methodology belongs to the class of arbitrary Lagrangian–Eulerian (ALE) methods [20, 14], which allows the motion of the mesh to be like either the Lagrangian or the Eulerian description of motion. Klingenberg and others developed an ALE-DG method for conservation laws [24, 15] and Hamilton–Jacobi equations [25], where local affine linear mappings connecting the cells for the current and next time level are defined and yield the time-dependent approximation space. The novelty of this method is that high order accuracy and stability can be proved under very mild conditions on mesh movements, in particular, no smoothness beyond Lipschitz continuity for the mesh movement function (which is assumed to be piecewise linear) is required [38, 32]. They also showed that the ALE-DG method satisfies the geometric conservation law (GCL) for any Runge–Kutta scheme, which is significant for the ALE method and has been analyzed by Guillard and Farhat [17]. The ALE-DG method shares many good properties of the DG method defined on static grids, e.g., the entropy stability, the local maximum principle, high order accuracy, and so on.

Solutions of hyperbolic equations often have the local structures, such as the discontinuities, so mesh adaptation has been an important tool in order to focus the computational effort where it is most needed. In the ALE-DG method, we want to relocate mesh point positions at each time level and do not change the number of mesh points. In such a way, more grid points should be clustered in the area with singularities to obtain better resolution compared with the DG method on the static mesh. This adaptive approach is the so-called r -adaptive method. In recent years, a few research works on this topic were published. Particularly, Tang and others proposed the r -adaptive algorithm to the DG method for conservation laws in [26, 31, 13], in which they still evolve the numerical solution on the same mesh to the upcoming time step, but a conservative remapping projection is needed on the new adaptive mesh at each time step.

It is worth pointing out that although many works have been done with adaptive mesh methods and DG methods separately, few works have combined adaptive mesh with DG methods to solve hyperbolic equations involving δ -singularities in an appropriate way without the need of remapping. In the ALE-DG method, after we get the mesh-redistribution at the next time level, the numerical solution will be evolved directly from the former time level to the next time level between two different meshes. We refer to Huang and Russell [22] and Li and Tang [26] for the adaptive mesh generation. However, due to the particularity of δ -singularities, we will adopt slightly different mesh density functions to obtain relatively smooth adaptive meshes.

It is well known that the numerical DG solution has spurious oscillations around this discontinuity, which is the so-called Gibbs phenomena. A simple example is the

following problem:

$$(1.2) \quad \begin{cases} u_t + u_x = 0, & (x, t) \in \Omega \times (0, T], \\ u(x, 0) = u_0(x), & x \in \Omega, \end{cases}$$

where the initial condition $u_0(x)$ contains δ -singularities but is otherwise smooth. Moreover, the problem (1.2) is periodic boundary condition, or the solution $u(x, t)$ has compact support when the reference domain Ω is \mathbb{R} . Given that $u_0(x) = \delta(x)$, the exact solution of (1.2) is discontinuous along the characteristic line $x = t$ and the DG solution has spurious oscillations around this discontinuous line, which produces the pollution region R_t . Yang and Shu in [34] have proved that the DG method on static grids for this problem can get high accuracy in the region apart from the pollution area, which is almost $\mathcal{O}(h^{\frac{1}{2}} \log(\frac{1}{h}))$ around the singularity. Besides, the negative-norm error estimate was also provided in the region apart from the pollution area ($\Omega \setminus R_t$) for the postprocessed approximation by convolving the DG solution with a suitable kernel. Detailed postprocessing techniques of the DG method for linear hyperbolic equation are given in [8].

In this work, the ALE-DG method will be employed to solve (1.1) on adaptive moving meshes. The ALE-DG method has been applied to hyperbolic conservation laws equations on moving mesh (cf. [24]), and high accuracy has been proved when the solution is smooth enough. We start from (1.2), develop the ALE-DG method, and prove the high accuracy and several negative norm estimates for the problem away from the pollution area. Similarly, we can perform the postprocessing technique on the moving mesh where the mesh is regular enough. Moreover, for the problem

$$(1.3) \quad \begin{cases} u_t + u_x = h(x, t), & (x, t) \in \Omega \times (0, T], \\ u(x, 0) = u_0(x), & x \in \Omega, \end{cases}$$

where the source term $h(x, t)$ contains δ -singularities, it can be proved that the above good performances we refer to still hold.

The outline of this paper is as follows. In section 2, we introduce the ALE-DG method for conservation laws and its L^2 stability. Section 3 is devoted to the L^2 norm and the negative norm error estimates for the singular initial condition problem (1.2). These estimates can be applied to the singular source problem (1.3) in section 4. Section 5 presents the methodology of adaptive moving mesh we use. In section 6, some numerical results are demonstrated to validate the accuracy and effectiveness of the ALE-DG scheme. Finally, some conclusions are given in section 7.

2. The ALE-DG method. We first take into account the moving mesh in order to describe the ALE-DG method. Assume points $\{x_{j-\frac{1}{2}}^n\}_{j=1}^N$ are the mesh points at time level t_n , so as $\{x_{j-\frac{1}{2}}^{n+1}\}_{j=1}^N$ at t_{n+1} , such that

$$(2.1) \quad \Omega = \bigcup_{j=1}^N [x_{j-\frac{1}{2}}^n, x_{j+\frac{1}{2}}^n], \quad \text{and} \quad \Omega = \bigcup_{j=1}^N [x_{j-\frac{1}{2}}^{n+1}, x_{j+\frac{1}{2}}^{n+1}].$$

Assume that the first point and the last point could move at the same speed for the periodic boundary problem and stay the same for the fixed boundary problem. Next, we define

$$(2.2) \quad w_{j-\frac{1}{2}} := \frac{x_{j-\frac{1}{2}}^{n+1} - x_{j-\frac{1}{2}}^n}{t_{n+1} - t_n}$$

as the moving speed of the j th mesh point from t_n to t_{n+1} . Then we define the function $w : \Omega \times [0, T] \rightarrow \mathbb{R}$ as the grid velocity. It is for any time-dependent cell $K_j(t) = [x_{j-\frac{1}{2}}(t), x_{j+\frac{1}{2}}(t)]$ and $t \in [t_n, t_{n+1}]$ given by

$$(2.3) \quad w(x, t) = w_{j+\frac{1}{2}} \frac{x - x_{j-\frac{1}{2}}(t)}{h_j(t)} + w_{j-\frac{1}{2}} \frac{x_{j+\frac{1}{2}}(t) - x}{h_j(t)},$$

where $h_j(t) = x_{j+\frac{1}{2}}(t) - x_{j-\frac{1}{2}}(t)$. In addition, we assume that $w(x, t)$ and $\partial_x w(x, t)$ are bounded in $\Omega \times [0, T]$. Denote the maximal cell length by

$$h := \max_{t \in [0, T]} \max_{1 \leq j \leq N} h_j(t).$$

We assume the mesh is regular, that is, there exists a constant $\sigma > 0$, independent of h , such that

$$(2.4) \quad h_j(t) \geq \sigma h \quad \forall j = 1, \dots, N.$$

Therefore, for any $t \in [t_n, t_{n+1}]$, the cell $K_j(t)$ can be connected with the reference cell $[-1, 1]$ by the time-dependent mapping

$$(2.5) \quad \chi_j : [-1, 1] \rightarrow K_j(t), \quad \chi_j(\xi, t) = \frac{h_j(t)}{2}(\xi + 1) + x_{j-\frac{1}{2}}(t).$$

Thus, we have

$$(2.6) \quad \partial_t(\chi_j(\xi, t)) = w(\chi_j(\xi, t), t) \quad \forall (\xi, t) \in [-1, 1] \times [t_n, t_{n+1}].$$

Furthermore, the finite-dimensional test function space is defined as

$$(2.7) \quad V_h := \{v_h \in L^2(\Omega) | v_h(\chi_j(\cdot, t)) \in \mathbb{P}^k([-1, 1]) \text{ } \forall t \in [t_n, t_{n+1}] \text{ and } j = 1, \dots, N\},$$

where $\mathbb{P}^k([-1, 1])$ denotes the space of polynomials in $[-1, 1]$ of degree at most k and the modal basis $\xi^j, j = 1, 2, \dots, k+1$ could be used in the reference cell. Moreover, we denote the L^2 inner products in $K_j(t)$ and Ω by $(v, w)_j := \int_{K_j(t)} v w dx$ and $(v, w) := \int_{\Omega} v w dx = \sum_j (v, w)_j$.

Next, we can easily get the transport equation in the approximation space V_h (cf. [24]).

LEMMA 2.1. *Let $u \in W^{1,\infty}(0, T; H^1(\Omega))$. Then for all test functions $v_h \in V_h$, where we can choose v_h as $\chi_j(\xi^i, t), i = 1, 2, \dots, k+1$, the following transport equation holds:*

$$(2.8) \quad \frac{d}{dt}(u, v_h)_j = (\partial_t u, v_h)_j + (\partial_x(uw), v_h)_j$$

$\forall j = 1, 2, \dots, N$, which is due to

$$(2.9) \quad \partial_t v_h(x, t) + w(x, t) \partial_x v_h(x, t) = 0.$$

We express the value of u on the left and right limits of the grid point $x_{j+\frac{1}{2}}(t)$ with $u_{j+\frac{1}{2}}^-$ and $u_{j+\frac{1}{2}}^+$, respectively, and indicate $g(\omega, u) = f(u) - \omega u$. Finally, we

obtain the following semidiscrete ALE-DG method for (1.1) by multiplying (1.1) with a test function $v_h \in V_h(t)$, using Lemma 2.1, and integrating by parts

$$(2.10) \quad \begin{aligned} \frac{d}{dt}(u_h, v_h)_j &= (g(\omega, u_h), \partial_x v_h)_j - \hat{g}(\omega_{j+\frac{1}{2}}, u_{h,j+\frac{1}{2}}^-, u_{h,j+\frac{1}{2}}^+)v_{h,j+\frac{1}{2}}^- \\ &\quad + \hat{g}(\omega_{j-\frac{1}{2}}, u_{h,j-\frac{1}{2}}^-, u_{h,j-\frac{1}{2}}^+)v_{h,j-\frac{1}{2}}^+ + (h(x, t), v_h)_j \end{aligned}$$

$\forall v_h \in V_h(t)$ and $j = 1, \dots, N$, where u_h is the approximation solution. In addition, the numerical flux $\hat{g}(\omega_{j+\frac{1}{2}}, u_{h,j+\frac{1}{2}}^-, u_{h,j+\frac{1}{2}}^+)$ should be chosen as a monotone numerical flux. Specifically, the ALE-DG method for the linear problem (1.2) is the following:

$$(2.11) \quad \begin{aligned} \frac{d}{dt}(u_h, v_h)_j &= (g(\omega, u_h), \partial_x v_h)_j - \hat{g}(\omega_{j+\frac{1}{2}}, u_{h,j+\frac{1}{2}}^-, u_{h,j+\frac{1}{2}}^+)v_{h,j+\frac{1}{2}}^- \\ &\quad + \hat{g}(\omega_{j-\frac{1}{2}}, u_{h,j-\frac{1}{2}}^-, u_{h,j-\frac{1}{2}}^+)v_{h,j-\frac{1}{2}}^+, \end{aligned}$$

where $g(\omega, u) = (1 - \omega)u$.

Define the jump and the mean of v at $x_{j-\frac{1}{2}}$ as $[v]_{j-\frac{1}{2}} = (v_{j-\frac{1}{2}}^+ - v_{j-\frac{1}{2}}^-)$ and

$$\{v\}_{j-\frac{1}{2}} = \frac{v_{j-\frac{1}{2}}^+ + v_{j-\frac{1}{2}}^-}{2}.$$

From Lemma 2.1, we can rewrite the scheme (2.10) as follows:

$$(2.12) \quad \begin{aligned} (\partial_t u_h, v_h)_j &= (\partial_x(\omega u_h), v_h)_j + (g(u_h), \partial_x v_h)_j - \hat{g}(\omega_{j+\frac{1}{2}}, u_{h,j+\frac{1}{2}}^-, u_{h,j+\frac{1}{2}}^+)v_{h,j+\frac{1}{2}}^- \\ &\quad + \hat{g}(\omega_{j-\frac{1}{2}}, u_{h,j-\frac{1}{2}}^-, u_{h,j-\frac{1}{2}}^+)v_{h,j-\frac{1}{2}}^+ \triangleq H_j(u_h, v_h). \end{aligned}$$

Summing up with respect to j , we obtain

$$(2.13) \quad \begin{aligned} (\partial_t u_h, v_h) &= -(\partial_x(\omega u_h), v_h) + (g(u_h), \partial_x v_h) \\ &\quad + \sum_j \hat{g}(\omega_{j-\frac{1}{2}}, u_{j-\frac{1}{2}}^-, u_{j-\frac{1}{2}}^+) [v_h]_{j-\frac{1}{2}} \triangleq H(u_h, v_h). \end{aligned}$$

For the convenience of theoretical analysis, we assume $1 - \omega$ dose not change its sign. Then we can choose the upwind numerical flux $\hat{g} = (1 - w)u_h^-$ if $1 - w > 0$ (if $1 - \omega < 0$, choosing $\hat{g} = (1 - \omega)u^+$). Integrating by parts, we have

$$(2.14) \quad H_j(u_h, v_h) = -(\partial_x u_h, v_h)_j - ((1 - w)[u_h]v_h^+)_{j-\frac{1}{2}}.$$

The cell entropy inequality and the L^2 stability of the ALE-DG scheme can be found in [24]. Here we recall the results, which will be used in our analysis.

LEMMA 2.2 (the L^2 -stability estimate of ALE-DG discretization). *Let u_h be the solution of the ALE-DG problem, where \hat{g} is the monotone flux. Then it holds that*

$$(2.15) \quad \|u_h(T)\| \leq \|u_h(0)\|.$$

Specially, for the linear conservation law (1.2), we have

$$(2.16) \quad \|u_h(T)\|^2 + 2 \int_0^T \sum_j \hat{g}(\hat{g}; u_h) [u_h]_{j-\frac{1}{2}}^2 dt = \|u_h(0)\|^2,$$

where

$$\hat{a}(\hat{g}; v) := \begin{cases} [v]^{-1}(g(\omega, \{v\}) - \hat{g}(\omega, v^-, v^+)) & \text{if } [v] \neq 0, \\ |g'(\omega, \{v\})| & \text{if } [v] = 0 \end{cases}$$

for any piecewise smooth function $v \in L^2$.

Moreover, Zhang and Shu (cf. [35]) proved the following lemma for the quantity $\hat{a}(\hat{g}; v)$.

LEMMA 2.3. *Suppose the numerical flux function \hat{g} is the monotone flux; then for any piecewise smooth function $v \in L^2(\Omega)$, the quantity $\hat{a}(\hat{g}; v)$ is nonnegative and bounded. In addition, we have*

$$\frac{1}{2}|g'(\omega, v)| \leq \hat{a}(\hat{g}; v) + C_*|[v]|,$$

where the positive constant C_* is the maximum of $|g''|$, which is zero for the linear problem (1.2).

Hence, by Lemma 2.2, for the linear problem, we have

$$(2.17) \quad 2 \int_0^T \sum_j \hat{a}(\hat{g}; u_h)_{j-\frac{1}{2}} [u_h]_{j-\frac{1}{2}}^2 dt \leq \|u_h(0)\|^2,$$

and then

$$(2.18) \quad \int_0^T \sum_j |1 - \omega_{j-\frac{1}{2}}| [u_h]_{j-\frac{1}{2}}^2 dt \leq \|u_h(0)\|^2.$$

3. Singular initial condition problem. In this section we consider the L^2 -norm and negative norm error estimates of the ALE-DG scheme (2.14) for (1.2). We first give some notation used throughout the paper.

3.1. Notation for functions spaces and projections. We first define some notation about norms. Denote $\|v\|_j$ and $\|v\|_{\infty,j}$ as the L^2 -norm and L^∞ -norm of v on K_j , respectively. Moreover,

$$\begin{aligned} \|v\|_{l,j} &= \left(\sum_{0 \leq \alpha \leq l} \|D^\alpha v\|_j^2 \right)^{\frac{1}{2}}, & \|v\|_{l,\infty,j} &= \max_{0 \leq \alpha \leq l} \|D^\alpha v\|_{\infty,j}, \\ \|v\|_l &= \left(\sum_j \|v\|_{l,j}^2 \right)^{\frac{1}{2}}, & \|v\|_{l,\infty} &= \max_j \|v\|_{l,\infty,j}, \\ \|v\|_\Gamma^2 &= \sum_j \left(|v_{j-\frac{1}{2}}^+|^2 + |v_{j-\frac{1}{2}}^-|^2 \right). \end{aligned}$$

The inverse properties of the finite space V_h will be used.

LEMMA 3.1. *When the mesh is regular, $\forall v \in V_h$, $\exists C > 0$, s.t.*

$$(3.1) \quad h^2 \|\partial_x v\|^2 + h \|v\|_\Gamma^2 \leq C \|v\|^2,$$

where the positive constant C is independent of h and v .

Define the L^2 -projection P_k , two Gauss–Radau projections P_- and P_+ of u into V_h as follows:

$$\begin{aligned} (P_k u, v_h) &= (u, v_h) \quad \forall v_h \in V_h \text{ with } v_h(\chi_j(., t)) \in P^k([-1, 1]), \\ (P_- u, v_h) &= (u, v_h) \quad \forall v_h \in V_h \text{ with } v_h(\chi_j(., t)) \in P^{k-1}([-1, 1]), \text{ and } (P_- u)_{j-\frac{1}{2}}^- = u_{j-\frac{1}{2}}^-, \\ (P_+ u, v_h) &= (u, v_h) \quad \forall v_h \in V_h \text{ with } v_h(\chi_j(., t)) \in P^{k-1}([-1, 1]), \text{ and } (P_+ u)_{j-\frac{1}{2}}^+ = u_{j-\frac{1}{2}}^+. \end{aligned}$$

The following lemma states the error of these projections [3].

LEMMA 3.2. *Let P_h be a projection, either P_k , P_- , or P_+ , and $P_h^\perp q = q - P_h q$ be the projection error. For any smooth function $q(x)$, $\exists c > 0$, such that*

$$(3.2) \quad \|P_h^\perp q\|_D + h\|\partial_x(P_h^\perp q)\|_D + h^{\frac{1}{2}}\|P_h^\perp q\|_{\infty, D} \leq ch^{k+1}|q|_{k+1, D},$$

$$(3.3) \quad \|P_h^\perp q\|_\Gamma \leq ch^{k+\frac{1}{2}}\|\partial_x^{k+1}q\|,$$

where the positive constant c is independent of h , solely depending on q , and D may be Ω or $K_j(t)$.

From [24], we have the following lemmas on the time-dependent projections.

LEMMA 3.3. *Let $\phi \in W^{1,\infty}(0, T; H^1(\Omega))$, and then it holds that*

$$(3.4) \quad \partial_t P_h \phi + \omega \partial_x P_h \phi = P_h(\partial_t \phi) + P_h(\omega \partial_x \phi).$$

LEMMA 3.4. *Let $u \in L^2(\Omega)$ and $v_h \in V_h$, and then it holds that*

$$(3.5) \quad (u - P_k u, \partial_t v_h)_j = 0.$$

3.2. L^2 -norm error estimate. We first state the L^2 -norm error estimate in the region away from the singularities and then give its proof.

THEOREM 3.5. *Let u be the exact solution of problem (1.2), where $u_0(x) \in C^{k+2}$ except the singularity $x = 0$. Assume u_h is the ALE-DG approximation and V_h is the space consisting of the k th piecewise polynomial ($k \geq 1$). Assuming $\partial_x w$, w are bounded and $(1-w)$ do not change its sign in $\Omega \times [0, T]$, we choose $\hat{g}(\omega, u_h) = g(\omega, u_h^-)$ as the upwind flux if $(1-w) \geq 0$. Then it holds that*

$$(3.6) \quad \|u(T) - u_h(T)\|_{\Omega \setminus R_T} \leq Ch^{k+1},$$

where C is a positive constant independent of h , and the pollution region R_T is $(T - C_* h^{\frac{1}{2}} \log(1/h), T + C_* h^{\frac{1}{2}} \log(1/h))$.

For simplicity, we assume that $u_0(x) = \delta(x) + f(x)$, where f is sufficiently smooth and periodic or has a compact support on the computational domain Ω . The proof of the theorem is based on [4], [36] involving the time-dependent approximation space. We start with some related contents.

3.2.1. The weight function. Let ϕ be a given positive bounded function, which can be called a weight function. For any function $v \in L^2$, we define the weighted L^2 -norm as

$$\|v\|_{\phi, D} = \left(\int_D v^2 \phi dx \right)^{\frac{1}{2}}$$

in the domain D . If $\phi = 1$ and $D = \Omega$, the corresponding subscript can be omitted. To obtain the $(k+1)$ th order accuracy in the L^2 -norm outside the pollution region,

we consider two weight functions $\phi^1(x, t)$ and $\phi^{-1}(x, t)$, which are used to determine the left-hand and right-hand boundaries of the pollution region R_T . Both weight functions are related to the cut-off of the exponential function $\varphi(r) \in C^1 : \Omega \rightarrow \mathbb{R}$,

$$\varphi(r) = \begin{cases} 2 - e^r, & r < 0, \\ e^{-r}, & r > 0. \end{cases}$$

The weight functions $\phi^a(x, t)$ for $a = \pm 1$ are defined as the solutions of the linear hyperbolic equation,

$$\begin{aligned} \phi_t^a + \phi_x^a &= 0, \\ \phi^a(x, 0) &= \varphi\left(\frac{a(x - x_c)}{\gamma h^\sigma}\right), \end{aligned}$$

where $\gamma > 0$, $0 < \sigma < 1$, and x_c are some parameters which will be chosen later. We always assume $\gamma h^{\sigma-1} \geq 1$ in this section. The properties of these two weight functions are given in [36]. Here, we list some of them that we will use.

PROPOSITION 3.6. *For each of the weight functions $\phi^a(x, t)$, the following properties hold:*

$$(3.7) \quad \begin{aligned} \max_{|d| \leq \gamma h^\sigma} \left| \frac{\partial_x^\alpha \phi^a(x + d, t)}{\partial_x^\alpha \phi^a(x, t)} \right| &\leq e, \alpha = 0, 1, 2; \\ |\partial_x^{\alpha+1} \phi^a(x, t)| &\leq \frac{1}{\gamma h^\sigma} \partial_x^\alpha \phi^a(x, t), \alpha = 0, 1, \end{aligned}$$

where $\partial_x^\alpha \phi^a$ are the spatial derivatives of ϕ^a with the order $\alpha \leq 0$; notice that $\partial_x^0 \phi^a = \phi^a$.

PROPOSITION 3.7. *For each of the weight functions $\phi^a(x, t)$, the following properties hold:*

$$(3.8) \quad \begin{aligned} 1 &\leq \phi^a(x, t) \leq 2, \quad a(x - x_c - t) \leq 0, \\ 0 &< \phi^a(x, t) < h^s, \quad a(x - x_c - t) > s \log(1/h) \gamma h^\sigma. \end{aligned}$$

LEMMA 3.8. *Let P_h be a Gauss–Radau projection, either P_- or P_+ . For any sufficiently smooth function $v(x)$ and any function $v_h \in V_h$, there exists a positive constant C independent of h and v , such that*

$$(3.9) \quad \begin{aligned} \|P_h^\perp v\|_{\phi, D} &\leq Ch^{k+1} \|\partial_x^{k+1} v\|_{\phi, D}, \\ \|\partial_x^\alpha P_h v\|_{\phi, D} &\leq Ch^{-\alpha} \|P_h v\|_{\phi, D}, \quad \alpha \geq 1, \\ \|P_h^\perp (\phi v_h)\|_{\phi^{-1}, D} &\leq C\gamma^{-1} h^{1-\sigma} \|v_h\|_{\phi, D}, \\ \|P_h (\phi v_h)\|_{\phi^{-1}, D} &\leq C \|v_h\|_{\phi, D}, \end{aligned}$$

where D is either the single cell K_j or the whole computational domain Ω .

In addition, we have the next two lemmas by simple computation.

LEMMA 3.9. *$\forall v \in V_h$, when choosing $\hat{g}(\omega, u_h) = g(\omega, u_h^-)$ as the upwind flux if $(1 - w) \geq 0$, we have*

$$(3.10) \quad H(v, \phi v) = \frac{1}{2} (v, \phi_x v) + \sum_j \left(\omega \phi v^+[v] - \frac{1}{2} \phi[v]^2 \right)_{j-\frac{1}{2}}.$$

LEMMA 3.10. For $u \in W^{1,\infty}(0, T; H^1(\Omega))$, when choosing $\hat{g}(\omega, u_h) = g(\omega, u_h^-)$ as the upwind flux if $(1-w) \geq 0$, $v \in V_h$, we obtain

$$(3.11) \quad H(v, P_+^\perp u) = 0,$$

$$(3.12) \quad H(P_-^\perp u, v) = \sum_j (\omega(P_-^\perp u)v)_{j-\frac{1}{2}}^+ = -(\partial_x(\omega(P_-^\perp u)v), 1).$$

3.2.2. Error representation and error equation. We first modify the initial condition $u_0(x) = \delta(x) + f(x)$ into $v_0(x)$, such that $v_0(x)$ satisfies

$$|\partial_x^\alpha v_0(x)| \leq Ch^{-\alpha-1}, \quad x \in I_{j_0},$$

and agrees with $u_0(x) \forall x \in \Omega \setminus I_{j_0}$, where I_{j_0} is the cell containing $x = 0$. Hence, we have

$$(3.13) \quad \|\partial_x^\alpha v_0(x)\| \leq Ch^{-\alpha-\frac{1}{2}}, \quad x \in I_{j_0}.$$

Then we define the following problem:

$$(3.14) \quad \begin{aligned} v_t + v_x &= 0, \\ v(x, 0) &= v_0(x), \end{aligned}$$

where v_0 is the initial solution of this problem.

Let $e = v - u_h$ be the error and u_h be the ALE-DG approximation to (1.2). We divide the error $e = \eta - \xi$, where

$$\eta = v - P_- v = P_-^\perp v \text{ and } \xi = u_h - P_- v.$$

Clearly, the error equation is $(e_t, v_h) = H(e, v_h) \forall v_h \in V_h(t)$. By the definition of ϕ and simple computation, we have

$$\begin{aligned} \frac{d}{dt} \|\xi\|_\phi^2 &= 2(\xi_t, \phi\xi) + (\xi^2, \partial_t \phi) + (\partial_x(\omega \xi^2 \phi), 1) \\ &= 2(\xi_t, \phi\xi) - (\xi, (\partial_x \phi)\xi) + (\partial_x(\omega \xi^2 \phi), 1) \\ &= 2(\xi_t, P_+^\perp(\phi\xi)) + 2(\xi_t, P_+(\phi\xi)) - (\xi, (\partial_x \phi)\xi) + (\partial_x(\omega \xi^2 \phi), 1). \end{aligned}$$

By Lemma 3.10,

$$\begin{aligned} (\xi_t, P_+(\phi\xi)) &= (\eta_t - e_t, P_+(\phi\xi)) \\ &= (\eta_t, P_+(\phi\xi)) - H(\eta, P_+(\phi\xi)) + H(\xi, P_+(\phi\xi)) \\ &= (\eta_t, P_+(\phi\xi)) + (\partial_x(\omega \eta P_+(\phi\xi)), 1) + H(\xi, \phi\xi). \end{aligned}$$

Then,

$$\begin{aligned} \frac{d}{dt} \|\xi\|_\phi^2 &= 2(\xi_t, P_+^\perp(\phi\xi)) + 2(\eta_t, P_+(\phi\xi)) + 2(\partial_x(\omega \eta P_+(\phi\xi)), 1) \\ &\quad + 2H(\xi, \phi\xi) - (\xi, (\partial_x \phi)\xi) + (\partial_x(\omega \xi^2 \phi), 1) \\ &= 2I_1 + 2I_2 - I_3, \end{aligned}$$

where

$$\begin{aligned} I_1 &= (\xi_t, P_+^\perp(\phi\xi)), \\ I_2 &= (\eta_t, P_+(\phi\xi)) + (\partial_x(\omega \eta P_+(\phi\xi)), 1), \\ I_3 &= -2H(\xi, \phi\xi) + (\xi, (\partial_x \phi)\xi) - (\partial_x(\omega \xi^2 \phi), 1). \end{aligned}$$

First, we estimate I_1 . Denote $q = \xi_t - P_{k-1}\xi_t$. From (2.14), we have

$$(e_t, q)_j = H_j(e, q) = -(\partial_x e, q)_j - ((1 - \omega)q^+[e])_{j-\frac{1}{2}}.$$

So, we have

$$(\xi_t, q)_j = (\eta_t, q)_j - (e_t, q)_j = (\eta_t, q)_j + (\partial_x(\eta - \xi), q)_j + ((1 - \omega)q^+[\eta - \xi])_{j-\frac{1}{2}}.$$

Integrating by parts, and from the definition of η and q , we also have

$$\begin{aligned} (\partial_x\eta, q)_j &= -(\eta, \partial_x q)_j - (\eta^+ q^+)_{j-\frac{1}{2}} = -(\eta^+ q^+)_{j-\frac{1}{2}} = -(q^+[\eta])_{j-\frac{1}{2}}, \\ (\partial_x\xi, q)_j &= 0, \end{aligned}$$

and

$$(\xi_t, q)_j = (\eta_t, q)_j - ((1 - \omega)q^+[\xi])_{j-\frac{1}{2}} + (\partial_x(\omega q\eta), 1)_j.$$

By the definition of η and Lemma 3.3, we have

$$(\eta_t, q)_j + (\partial_x(\omega q\eta), 1)_j = (P_-^\perp(\partial_t v + \omega \partial_x v), q)_j + ((\partial_x \omega)\eta, q)_j + (\omega \eta, \partial_x q)_j.$$

Thus

$$(\xi_t, q)_j = (P_-^\perp((\omega - 1)\partial_x v), q)_j + ((\partial_x \omega)\eta, q)_j + (\eta, \omega \partial_x q)_j - ((1 - \omega)q^+[\xi])_{j-\frac{1}{2}}.$$

Next, we estimate I_1 and define $\psi = \sqrt{\phi}$. From Proposition 3.6 and Lemmas 3.1 and 3.8, we get

$$\begin{aligned} (\xi_t, P_+^\perp(\phi\xi))_j &= \left(\frac{(\xi_t, q)_j}{\|q\|_j^2} q, P_+^\perp(\phi\xi) \right)_j \\ &= \left((P_-^\perp((\omega - 1)\partial_x v), q)_j + ((\partial_x \omega)\eta, q)_j + (\eta, \omega \partial_x q)_j \right. \\ &\quad \left. - ((1 - \omega)q^+[\xi])_{j-\frac{1}{2}} \right) \frac{q}{\|q\|_j^2}, P_+^\perp(\phi\xi) \Big)_j \\ &\leq \frac{c}{\|q\|_j} (|\psi P_-^\perp((\omega - 1)\partial_x v), q)_j| + |(\psi(\partial_x \omega)\eta, q)_j| \\ &\quad + |(\psi\eta, (\omega - \omega_{j-\frac{1}{2}})\partial_x q)_j| \|P_+^\perp(\phi\xi)\|_{\phi^{-1}, j} \\ &\quad + \frac{c}{\|q\|_j} |(1 - \omega)[\psi\xi]q^+|_{j-\frac{1}{2}} \|P_+^\perp(\phi\xi)\|_{\phi^{-1}, j} \\ &\leq \frac{ch^{1-\sigma}}{\gamma} \left(\|P_-^\perp((\omega - 1)\partial_x v)\|_{\phi, j}^2 + \|\eta\|_{\phi, j}^2 + \|\xi\|_{\phi, j}^2 \right) \\ &\quad + \frac{ch^{\frac{1}{2}-\sigma}}{\gamma} (((1 - \omega)\phi[\xi]^2)_{j-\frac{1}{2}} + \|\xi\|_{\phi, j}^2). \end{aligned}$$

Summing up with respect to j , we obtain

$$\begin{aligned} &(\xi_t, P_+^\perp(\phi\xi)) \\ &\leq \frac{ch^{1-\sigma}}{\gamma} (\|P_-^\perp((\omega - 1)\partial_x v)\|_\phi^2 + \|\eta\|_\phi^2 + \|\xi\|_\phi^2) + \frac{ch^{\frac{1}{2}-\sigma}}{\gamma} \left(\sum_j ((1 - \omega)\phi[\xi]^2)_{j-\frac{1}{2}} + \|\xi\|_\phi^2 \right). \end{aligned}$$

Second, we estimate I_2 by Lemmas 3.3 and 3.8.

$$\begin{aligned}
I_2 &= (\eta_t, P_+(\phi\xi)) + (\partial_x(\omega\eta P_+(\phi\xi)), 1) \\
&= (P_-^\perp(\partial_t v + \omega\partial_x v) - \omega\partial_x\eta, P_+(\phi\xi)) + ((\partial_x\omega)\eta, P_+(\phi\xi)) \\
&\quad + (\omega(\partial_x\eta), P_+(\phi\xi)) + (\omega\eta, \partial_x P_+(\phi\xi)) \\
&= (P_-^\perp((\omega - 1)\partial_x v), P_+(\phi\xi)) + ((\partial_x\omega)\eta, P_+(\phi\xi)) + \sum_j (\eta, (\omega - \omega_{j-\frac{1}{2}})\partial_x P_+(\phi\xi))_j \\
&\leq c(\|P_-^\perp((\omega - 1)\partial_x v)\|_\phi \|\xi\|_\phi + \|\eta\|_\phi \|\xi\|_\phi + \|\eta\|_\phi h \|\partial_x P_+(\phi\xi)\|_{\phi^{-1}}) \\
&\leq c(\|P_-^\perp((\omega - 1)\partial_x v)\|_\phi^2 + \|\xi\|_\phi^2 + \|\eta\|_\phi^2).
\end{aligned}$$

Finally, we estimate I_3 from Lemma 3.9.

$$\begin{aligned}
I_3 &= -2H(\xi, \phi\xi) + (\xi, (\partial_x\phi)\xi) - (\partial_x(\omega\xi^2\phi), 1) \\
&= -(\xi, \phi_x\xi) - \sum_j 2(\omega\phi\xi^+[\xi] - \frac{1}{2}\phi[\xi]^2)_{j-\frac{1}{2}} + (\xi, (\partial_x\phi)\xi) + \sum_j [\omega\xi^2\phi]_{j-\frac{1}{2}} \\
&= -\sum_j (2\omega\phi(\xi^+ - \{\xi\})[\xi])_{j-\frac{1}{2}} + \sum_j (\phi[\xi]^2)_{j-\frac{1}{2}} \\
&= \sum_j ((1 - \omega)\phi[\xi]^2)_{j-\frac{1}{2}}.
\end{aligned}$$

Then γ is large enough and $\sigma = \frac{1}{2}$, and we have

$$\frac{d}{dt} \|\xi\|_\phi^2 = 2I_1 + 2I_2 - I_3 \leq c(\|P_-^\perp((\omega - 1)\partial_x v)\|_\phi^2 + \|\eta\|_\phi^2 + \|\xi\|_\phi^2).$$

By Gronwall's inequality, we obtain

$$(3.15) \quad \|\xi(T)\|_\phi^2 \leq c \int_0^T (\|P_-^\perp((\omega - 1)\partial_x v)\|_\phi^2 + \|\eta\|_\phi^2) dt + c\|\xi(0)\|_\phi^2.$$

3.2.3. The final estimate. This part is similar to [4], [36]. We will only analyze the left-hand boundary of R_T because the analysis of the right one is analogous. Denote $x_L(t) = t + x_c$ with

$$x_c = -2s \log(1/h)\gamma h^\sigma,$$

where s and γ is large enough and $\sigma = \frac{1}{2}$. As we have mentioned before, the δ -singularity is contained in the cell I_{j_0} at initial time. Then by Proposition 3.7, we can obtain $0 < \phi(x) < h^s$ for any $x \in I_{j_0}$.

1. We choose v_0 to satisfy $P_k v_0 = P_k u_0 = u_h(0)$. By Lemma 3.8, Proposition 3.7, Lemma 3.2, and (3.13), then we have

$$\begin{aligned}
\|\xi(0)\|_\phi &= \|u_h(0) - P_- v_0\|_\phi = \|P_k v_0 - v_0 + v_0 - P_- v_0\|_\phi \\
&\leq \|P_k v_0 - v_0 + v_0 - P_- v_0\|_{\phi, L^2(R \setminus I_{j_0})} \\
&\quad + \|P_k v_0 - v_0 + v_0 - P_- v_0\|_{\phi, L^2(I_{j_0})} \\
&\leq ch^{k+1} \|f\|_{k+1} + ch^{\frac{(s-1)}{2}}.
\end{aligned}$$

If s is sufficiently large, then $\|\xi(0)\|_\phi \leq Ch^{k+1}$.

2. Define the domain $R_T^+ = (x_L(T), \infty)$, and then we have

$$\|u_h - v\|_{R \setminus R_T^+} \leq \|u_h - v\|_{\phi, R \setminus R_T^+} \leq \|\eta\|_{\phi, R \setminus R_T^+} + \|\xi\|_{\phi} \leq ch^{k+1} \|f\|_{k+1} + \|\xi\|_{\phi}.$$

To estimate $\|\xi\|_{\phi}$, we need to use (3.15). Denote

$$x_{\omega}(t) = \max\{x_{j+\frac{1}{2}} : x_{j-\frac{1}{2}} < t + \frac{1}{2}x_c \ \forall j\}$$

and $R_1(t) = (-\infty, x_{\omega}(t))$, $R_2 = R \setminus R_1(t) = (x_{\omega}(t), \infty)$. If $\gamma h^{\sigma-1}$ is large enough, $R_1(t)$ stays away from the bad interval $[t-h, t+h]$, where $v(x, t) \neq u(x, t)$, and then we have

$$\begin{aligned} \|P_-^\perp((\omega-1)\partial_x v)\|_{\phi, R_1(t)} &\leq ch^{k+1}|(\omega-1)\partial_x f|_{k+1} \leq ch^{k+1}\|f\|_{k+2}, \\ \|\eta\|_{\phi, R_1(t)} &\leq ch^{k+1}|f|_{k+1} \leq ch^{k+1}\|f\|_{k+2}, \end{aligned}$$

where R_2 contains the whole pollution region, and we can use the weight function. By Proposition 3.7, we have $\phi \leq h^s$ in R_2 . Then we obtain

$$\begin{aligned} \|P_-^\perp((\omega-1)\partial_x v)\|_{\phi, R_2(t)} &\leq ch^{\frac{s}{2}}\|P_-^\perp((\omega-1)\partial_x v)\|_{R_2(t)} \\ &\leq ch^{\frac{s}{2}+k+1}\|v\|_{k+2, R_2(t)} \\ &\leq ch^{\frac{s-3}{2}} + ch^{\frac{s}{2}+k+1}\|f\|_{k+2, R_2(t)} \end{aligned}$$

and

$$\|\eta\|_{\phi, R_2(t)} \leq ch^{\frac{s}{2}}\|\eta\|_{R_2(t)} \leq ch^{\frac{s}{2}+k+1}|v|_{k+1, R_2(t)} \leq ch^{\frac{s-1}{2}} + ch^{\frac{s}{2}+k+1}\|f\|_{k+1}.$$

If we take s large enough, we have

$$\|u_h - u\|_{R \setminus R_T^+} = \|u_h - v\|_{R \setminus R_T^+} \leq ch^{k+1}\|f\|_{k+2} + ch^{\frac{s-3}{2}} \leq ch^{k+1}.$$

Similarly, we can estimate the right-hand side of the nonsmooth region.

3.3. Negative norm error estimates. In this section, we still consider the problem(1.2) and $u_0(x) = \delta(x)$ for simplicity. We mainly focus on the negative norm error estimate and introduce the postprocessing technique in brief. Next, we state the following three theorems and give their proofs.

THEOREM 3.11. *$u(T)$ is the exact solution of problem (1.2) at $t = T$, and u_h is the approximation for the ALE-DG discretization. We choose $\hat{g}(w, u_h)$ as a monotone flux, and then*

$$\|u(T) - u_h(T)\|_{-(k+1)} \leq ch^k,$$

where we denote the negative norm by $\|u(T) - u_h(T)\|_{-(k+1)} = \sup_{\Phi \in C_0^\infty(\Omega)} \frac{(u(T) - u_h(T), \Phi)}{\|\Phi\|_{k+1}}$.

Proof. For $\Phi \in C_0^\infty(\Omega)$, by duality, we have

$$\begin{cases} \phi_t + \phi_x = 0, & (x, t) \in \Omega \times [0, T], \\ \phi(x, T) = \Phi(x), & x \in \Omega, \end{cases}$$

and

$$\begin{aligned} ((u - u_h)(T), \Phi) &= (u, \phi)(T) - (u_h, \phi)(T) \\ &= (u, \phi)(0) - (u_h, \phi)(0) - \int_0^T \frac{d}{dt}(u_h, \phi) dt \\ &= (u - u_h, \phi)(0) - \int_0^T \{(\partial_t u_h, \phi) + (u_h, \partial_t \phi) + (\partial_x(\omega u_h \phi), 1)\} dt. \end{aligned}$$

For $q \in V_h$, we have

$$\begin{aligned} (\partial_t u_h, \phi) &= (\partial_t u_h, \phi - q) + (\partial_t u_h, q) \\ &= (\partial_t u_h, \phi - q) + H(u_h, q) \\ &= (\partial_t u_h, \phi - q) - H(u_h, \phi - q) + H(u_h, \phi). \end{aligned}$$

Define

$$\begin{aligned} \theta_M &= (u - u_h, \phi)(0), \\ \theta_N &= \int_0^T \{(\partial_t u_h, \phi - q) - H(u_h, \phi - q)\} dt, \\ \theta_C &= \int_0^T \{H(u_h, \phi) + (u_h, \partial_t \phi) + (\partial_x(\omega u_h \phi), 1)\} dt. \end{aligned}$$

Hence, $((u - u_h)(T), \Phi) = \theta_M - \theta_N - \theta_C \leq |\theta_M| + |\theta_N| + |\theta_C|$.

(1) Estimate for the initial error θ_M .

We assume only I_{j_0} contains $\delta(x)$ -singularity $x = 0$ and $u_h = P_k u(x, 0)$ is the L^2 -projection of $u(x, 0)$ to V_h . We can obtain $\|u_h\|_{L^2} \leq ch^{-\frac{1}{2}}$, and then

$$\begin{aligned} |(u - u_h, \phi)_{j_0}| &= |(u - u_h, \phi - P_k \phi)_{j_0}| = |(u, \phi - P_k \phi)_{j_0}| \\ &\leq \|\phi - P_k \phi\|_{\infty, I_{j_0}} \\ &\leq ch^{k+\frac{1}{2}} |\phi|_{k+1, I_{j_0}}. \end{aligned}$$

When $j \neq j_0$, I_j does not contain $\delta(x)$ -singularity (u is smooth in I_j), and thus

$$|(u - u_h, \phi)_j| = |(u - P_k u, \phi - P_k \phi)_j| \leq ch^{2k+2} |u_0|_{k+1,j} |\phi|_{k+1,j}.$$

(2) Estimate for the consistency error θ_C .

$$\begin{aligned} &H(u_h, \phi) + (u_h, \partial_t \phi) + (\partial_x(\omega u_h \phi), 1) \\ &= -(\partial_x(\omega u_h), \phi) + ((u_h - \omega u_h), \partial_x \phi) \\ &\quad + \sum_j \hat{g}[\phi]_{j-\frac{1}{2}} + (u_h, -\partial_x \phi) + (\omega u_h, \partial_x \phi) + (\partial_x(\omega u_h), \phi) \\ &= \sum_j \hat{g}[\phi]_{j-\frac{1}{2}} = 0. \end{aligned}$$

(3) Estimate for the residual error θ_N .

Choosing the test function $q = P_k \phi$, by Lemma 3.4, the Cauchy–Schwarz inequality, and Lemma 2.3, it follows that

$$\begin{aligned}
& |(\partial_t u_h, \phi - q) - H(u_h, \phi - q)| \\
&= \left| (\partial_t u_h, \phi - P_k \phi) + (\partial_x(\omega u_h), \phi - P_k \phi) - (g(u_h), \partial_x(\phi - P_k \phi)) \right. \\
&\quad \left. - \sum_j \hat{g}[\phi - P_k \phi]_{j-\frac{1}{2}} \right| \\
&= \left| (\partial_t u_h, P_k^\perp \phi) + (\partial_x(\omega u_h), P_k^\perp \phi) + (\partial_x(u_h - \omega u_h), P_k^\perp \phi) \right. \\
&\quad \left. + \sum_j [g(u_h) P_k^\perp \phi]_{j-\frac{1}{2}} - \sum_j \hat{g}[P_k^\perp \phi]_{j-\frac{1}{2}} \right| \\
&= \left| (\partial_t u_h, P_k^\perp \phi) + (\partial_x u_h, P_k^\perp \phi) + \sum_j (\{g(u_h)\} [P_k^\perp \phi]_{j-\frac{1}{2}} \right. \\
&\quad \left. + [g(u_h)] \{P_k^\perp \phi\}_{j-\frac{1}{2}} - \hat{g}[P_k^\perp \phi]_{j-\frac{1}{2}}) \right| \\
&= \left| \sum_j (g(\omega_{j-\frac{1}{2}}, \{u_h\}_{j-\frac{1}{2}}) - \hat{g}_{j-\frac{1}{2}}) [P_k^\perp \phi]_{j-\frac{1}{2}} + \sum_j [(1-\omega) u_h]_{j-\frac{1}{2}} \{P_k^\perp \phi\}_{j-\frac{1}{2}} \right| \\
&= \left| \sum_j \hat{a}(\hat{g}_{j-\frac{1}{2}}; (u_h)_{j-\frac{1}{2}}) [u_h]_{j-\frac{1}{2}} [P_k^\perp \phi]_{j-\frac{1}{2}} + \sum_j (1-\omega_{j-\frac{1}{2}}) [u_h]_{j-\frac{1}{2}} \{P_k^\perp \phi\}_{j-\frac{1}{2}} \right| \\
&\leq \left(\sum_j \hat{a}(\hat{g}_{j-\frac{1}{2}}; (u_h)_{j-\frac{1}{2}})^2 [u_h]_{j-\frac{1}{2}}^2 \right)^{\frac{1}{2}} \left(\sum_j [P_k^\perp \phi]_{j-\frac{1}{2}}^2 \right)^{\frac{1}{2}} \\
&\quad + \left(\sum_j (1-\omega_{j-\frac{1}{2}})^2 [u_h]_{j-\frac{1}{2}}^2 \right)^{\frac{1}{2}} \left(\sum_j \{P_k^\perp \phi\}_{j-\frac{1}{2}}^2 \right)^{\frac{1}{2}} \\
&\leq ch^{k+\frac{1}{2}} |\phi|_{k+1} \left(\sum_j \hat{a}(\hat{g}_{j-\frac{1}{2}}; (u_h)_{j-\frac{1}{2}}) [u_h]_{j-\frac{1}{2}}^2 \right)^{\frac{1}{2}}.
\end{aligned}$$

By the Cauchy–Schwarz inequality and Lemma 2.2, we have

$$\begin{aligned}
|\theta_N| &\leq ch^{k+\frac{1}{2}} |\phi|_{k+1} \int_0^T \left(\sum_j \hat{a}[u_h]_{j-\frac{1}{2}}^2 \right)^{\frac{1}{2}} dt \\
&\leq ch^{k+\frac{1}{2}} |\phi|_{k+1} T^{\frac{1}{2}} \left(\int_0^T \sum_j \hat{a}[u_h]_{j-\frac{1}{2}}^2 dt \right)^{\frac{1}{2}} \\
&\leq ch^{k+\frac{1}{2}} T^{\frac{1}{2}} \|u_h\| |\phi|_{k+1} \\
&\leq ch^k T^{\frac{1}{2}} |\phi|_{k+1}.
\end{aligned}$$

Combining the above, we obtain

$$\begin{aligned}
\|u - u_h\|_{-(k+1), \Omega} &= \sup_{\Phi \in C_0^\infty(\Omega)} \frac{(u(T) - u_h(T), \Phi)}{\|\Phi\|_{k+1}} \leq \sup_{\Phi \in C_0^\infty(\Omega)} \frac{|\theta_N| + |\theta_M|}{\|\Phi\|_{k+1}} \\
&\leq ch^k T^{\frac{1}{2}} + ch^{k+\frac{1}{2}} \leq ch^k.
\end{aligned}$$

□

THEOREM 3.12. *When $(1 - \omega)$ does not change its sign, we may as well assume $1 - \omega > 0$ and choose \hat{g} as the upwind flux, $\hat{g}(\omega, u) = (1 - \omega)u^- = g(\omega, u^-)$. Then we have*

$$(3.16) \quad \|u(T) - u_h(T)\|_{-(k+2), \Omega} \leq ch^{k+\frac{1}{2}}.$$

Proof. Choosing $q = P_+^\perp \phi$, we compute $\theta_N = \int_0^T (\partial_t u_h, P_+^\perp \phi) - H(u_h, P_+^\perp \phi) dt$. By the definition of the operator P_+ and integration by parts, we have

$$\begin{aligned} H(u_h, P_+^\perp \phi) &= -(\partial_x(\omega u_h), P_+^\perp \phi) + (g(u_h), \partial_x P_+^\perp \phi) + \sum_j \hat{g}(\omega, u_h) [P_+^\perp \phi]_{j-\frac{1}{2}} \\ &= -(\partial_x(\omega u_h), P_+^\perp \phi) - (\partial_x g(u_h), P_+^\perp \phi) - \sum_j [g(u_h) P_+^\perp \phi]_{j-\frac{1}{2}} \\ &\quad + \sum_j \hat{g}(\omega, u_h) [P_+^\perp \phi]_{j-\frac{1}{2}} \\ &= -(\partial_x u_h, P_+^\perp \phi) - \sum_j [g(\omega, u_h) P_+^\perp \phi]_{j-\frac{1}{2}} - \sum_j g(\omega, u_h^-) (P_+^\perp \phi)_{j-\frac{1}{2}}^- \\ &= \sum_j g(\omega, u_h^-) (P_+^\perp \phi)_{j-\frac{1}{2}}^- - \sum_j g(\omega, u_h^-) (P_+^\perp \phi)_{j-\frac{1}{2}}^- \\ &= 0. \end{aligned}$$

Hence,

$$\begin{aligned} (\partial_t u_h, P_+^\perp \phi) &= \frac{d}{dt}(u_h, P_+^\perp \phi) - (u_h, \partial_t P_+^\perp \phi) - (\partial_x(\omega u_h P_+^\perp \phi), 1), \\ \int_0^T (\partial_t(u_h), P_+^\perp \phi) &= (u_h, P_+^\perp \phi)(T) - (u_h, P_+^\perp \phi)(0) \\ &\quad - \int_0^T \{(u_h, \partial_t P_+^\perp \phi) + (\partial_x(\omega u_h P_+^\perp \phi), 1)\} dt. \end{aligned}$$

And then, by Lemma 3.3, it follows that

$$\begin{aligned} &(u_h, \partial_t P_+^\perp \phi) + (\partial_x(\omega u_h P_+^\perp \phi), 1) \\ &= (u_h, P_+^\perp (\partial_t \phi + \omega \partial_x \phi) - \omega \partial_x(P_+^\perp \phi)) + ((\partial_x \omega) u_h, P_+^\perp \phi) \\ &\quad + (\omega \partial_x u_h, P_+^\perp \phi) + (\omega u_h, \partial_x(P_+^\perp \phi)) \\ &= (u_h, P_+^\perp ((\omega - 1) \partial_x \phi)) + ((\partial_x \omega) u_h, P_+^\perp \phi) + (\omega \partial_x u_h, P_+^\perp \phi). \end{aligned}$$

By the property of projection, $\max_x |\partial_x w| \leq c_1$, the Cauchy–Schwarz inequality, and Lemmas 3.1, and 2.2, we obtain that

$$\begin{aligned} (\omega \partial_x u_h, P_+^\perp \phi) &= \sum_j (\omega \partial_x u_h, P_+^\perp \phi)_{K_j(t)} = \sum_j ((\omega - \omega_{j-\frac{1}{2}}) \partial_x u_h, P_+^\perp \phi)_{K_j(t)} \\ &\leq \sum_j c_1 h \|\partial_x u_h\|_{K_j(t)} \|P_+^\perp \phi\|_{K_j(t)} \leq ch \|\partial_x u_h\| \|P_+^\perp \phi\| \\ &\leq c \|u_h\| \|P_+^\perp \phi\| \leq \|u_h(0)\| \|P_+^\perp \phi\|. \end{aligned}$$

By the Cauchy–Schwarz inequality and Lemmas 2.2 and 3.2, we can see

$$\begin{aligned}
\theta_N &= \int_0^T (\partial_t u_h, P_+^\perp \phi) \\
&\leq \|u_h(0)\|(\|(P_+^\perp \phi)(0)\| + \|(P_+^\perp \phi)(T)\|) \\
&\quad + c \int_0^T \|u_h(0)\|(\|P_+^\perp((\omega - 1)\partial_x \phi)\| + \|P_+^\perp \phi\|) dt \\
&\leq c \|u_h(0)\| \left(h^{k+1} |\Phi|_{k+1} + \int_0^T h^{k+1} \|\Phi\|_{k+2} dt \right) \\
&\leq c(1+T)h^{k+1} \|u_h(0)\| \|\Phi\|_{k+2}.
\end{aligned}$$

Finally we obtain

$$\begin{aligned}
\|u(T) - u_h(T)\|_{-(k+2)} &= \sup_{\Phi \in C_0^\infty(\Omega)} \frac{(u(T) - u_h(T), \Phi)}{\|\Phi\|_{k+2}} \\
&\leq \sup_{\Phi \in C_0^\infty(\Omega)} \frac{ch^{k+\frac{1}{2}} |\Phi|_{k+1} + c(1+T)h^{k+\frac{1}{2}} \|\Phi\|_{k+2}}{\|\Phi\|_{k+2}} \\
&\leq c(1+T)h^{k+\frac{1}{2}}. \quad \square
\end{aligned}$$

THEOREM 3.13. *By the assumptions of Theorem 3.5, we can obtain the following:
 $\forall \Omega_1 \subset \subset \Omega \setminus R_T$,*

$$(3.17) \quad \|u(T) - u_h(T)\|_{-(k+1), \Omega_1} \leq ch^{2k+1}.$$

Proof. The proof follows from

$$\begin{aligned}
\|u(T) - u_h(T)\|_{-(k+1), \Omega_1} &= \sup_{\Phi \in C_0^\infty(\Omega_1)} \frac{(u(T) - u_h(T), \Phi)_{\Omega_1}}{\|\Phi\|_{k+1, \Omega_1}} \\
&= \sup_{\Phi \in C_0^\infty(\Omega_1)} \frac{(u(T) - u_h(T), \Phi)}{\|\Phi\|_{k+1}}.
\end{aligned}$$

The proof is similar to Theorem 3.11, and we have

$$(u(T) - u_h(T), \Phi) \leq |\theta_M| + |\theta_N|,$$

$$|\theta_M| \leq ch^{2k+2} |\phi|_{k+1} \leq ch^{2k+2} \|\Phi\|_{k+1},$$

$$|\theta_N| = \left| \int_0^T \sum_j \hat{a}(\hat{g}; u_h) [u_h]_{j-\frac{1}{2}} [P_k^\perp \phi]_{j-\frac{1}{2}} + \sum_j (1 - \omega_{j-\frac{1}{2}}) [u_h]_{j-\frac{1}{2}} \{P_k^\perp \phi\}_{j-\frac{1}{2}} dt \right|.$$

We may as well assume $u \in C(\Omega)$, since only one interval contains an δ -singularity for an exact solution. Actually, we can correct the exact solution to v such that u_h

keeps invariant and v is also smooth as in section 3.2. Then we have

$$\begin{aligned}
& \left| \sum_j \hat{a}[u_h][P_k^\perp \phi] + \sum_j (1 - \omega)[u_h]\{P_k^\perp \phi\} \right| \\
&= \left| \sum_j \hat{a}[u_h - P_k u + P_k u - u][P_k^\perp \phi] + \sum_j (1 - \omega)[u_h - P_k u + P_k u - u]\{P_k^\perp \phi\} \right| \\
&\leq c \left(\sum_j [u_h - P_k u]^2 \right)^{\frac{1}{2}} \left(\sum_j [P_k^\perp \phi]^2 \right)^{\frac{1}{2}} + c \left(\sum_j [P_k u - u]^2 \right)^{\frac{1}{2}} \left(\sum_j [P_k^\perp \phi]^2 \right)^{\frac{1}{2}} \\
&\quad + c \left(\sum_j [u_h - P_k u]^2 \right)^{\frac{1}{2}} \left(\sum_j \{P_k^\perp \phi\}^2 \right)^{\frac{1}{2}} + c \left(\sum_j [P_k u - u]^2 \right)^{\frac{1}{2}} \left(\sum_j \{P_k^\perp \phi\}^2 \right)^{\frac{1}{2}} \\
&\leq ch^{k+\frac{1}{2}} |\phi|_{k+1} h^{-\frac{1}{2}} (\|u_h - P_k u\|_{\Omega_1} + \|P_k u - u\|_{\Omega_1}) \\
&\leq ch^k |\phi|_{k+1} (\|u - P_k u\|_{\Omega_1} + \|u - u_h\|_{\Omega_1}) \\
&\leq ch^k |\phi|_{k+1} (h^{k+1} + \|u - u_h\|_{\Omega_1}).
\end{aligned}$$

Until now, we have had

$$|\theta_N| \leq ch^k |\phi|_{k+1} (h^{k+1} + \|u - u_h\|_{\Omega_1}),$$

and it holds for monotone fluxes. Next, from Theorem 3.5, we obtain

$$|\theta_N| \leq ch^{2k+1} |\phi|_{k+1}.$$

From above, we can see

$$(u(T) - u_h(T), \Phi) \leq ch^{2k+2} \|\Phi\|_{k+1} + ch^{2k+1} |\Phi|_{k+1},$$

so

$$\|u(T) - u_h(T)\|_{-(k+1), \Omega_1} \leq ch^{2k+1}. \quad \square$$

Note that the assumption of this theorem is for the upwind flux.

3.4. Postprocessing technique. We can still proceed with the general postprocessing technique in the nonuniform mesh, which was first demonstrated by Bramble and Schatz [1] to obtain a better approximation. The postprocessing solution is given by

$$(3.18) \quad u_h^*(x) = K_H^{(r+1, k+1)} * u_h(x),$$

where the operator $K^{(r+1, k+1)}$ is a linear combination of the $(k+1)$ th degree central B-splines,

$$(3.19) \quad K^{(r+1, k+1)}(x) = \sum_{\gamma=0}^r k_\gamma^{(r+1, k+1)} \psi^{(k+1)} \left(x + \frac{r}{2} - \gamma \right),$$

and $K_H^{(r+1, k+1)}$ is given by $K_H^{(r+1, k+1)}(x) = K^{(r+1, k+1)}(\frac{x}{H})/H$. Let the number of B-splines be $r+1 = 2k+1$. $k_\gamma^{(r+1, k+1)}$ can be calculated by the requirement

$$K^{(r+1, k+1)} * p = p, \quad p = 1, x, \dots, x^r.$$

Besides, we define recursively the central B-splines as

$$(3.20) \quad \begin{aligned} \psi^{(1)}(x) &= \chi_{(-\frac{1}{2}, \frac{1}{2})}(x), \\ \psi^{(l+1)}(x) &= \psi^{(1)}(x) * \psi^{(l)}(x), \quad l \geq 1. \end{aligned}$$

Moreover, we have the error estimate from [8].

THEOREM 3.14. *Let U be a function in $L^2(\Omega_1)$, where Ω_1 is an open set in R^1 , and let u be a function in $H^\nu(\Omega_1)$. Let Ω_0 be an open set in R^1 such that $\Omega_0 + 2\text{supp}(K_H^{(\nu, l)}) \subseteq \Omega_1 \forall H \leq H_0$. Then, for $H \leq H_0$, we have*

$$(3.21) \quad \|u - K_H^{(\nu, l)} * U\|_{0, \Omega_0} \leq \frac{H^\nu}{\nu!} C_1 |u|_{\nu, \Omega_1} + C_1 C_2 \sum_{|\alpha| \leq l} \|\partial_H^\alpha(u - U)\|_{-l, \Omega_1},$$

where $C_1 = \sum_\gamma |k_\gamma^{\nu, l}|$ and C_2 depends solely on Ω_0, Ω_1, ν , and l .

Let u_h be the ALE-DG approximate solution, $\Omega_1 = \Omega \setminus R_T$, and u be the exact solution. By Theorem 3.14, the error $\|u - K_H^{(\nu, l)} * u_h\|_{0, \Omega_0}$ depends on $|u|_{\nu, \Omega_1}$ and $\|\partial_H^\alpha(u - u_h)\|_{-l, \Omega_1}$. It is difficult to obtain $\|\partial_H^\alpha(u - u_h)\|_{-l, \Omega_1}$ for general nonuniform meshes even if we have Theorem 3.13.

But, in section 6, we can observe the $(2k + 1)$ th superconvergence numerically in the smooth region. Besides, we choose the local mesh size h_j as the scaling H for nonuniform meshes. Because of the mesh nonuniform, position-dependent filters need to be used to handle boundary regions so that the support of the filter remains inside the domain. See [27] for more details.

4. Singular source term problem. In this section, we discuss the error estimates for linear hyperbolic conservation laws with a source term. For simplicity, we only consider problem (1.3), where $h(x, t) = \delta(x)$ and $u_0(x) = 0$. Otherwise, we apply Duhamel's principle to deal with this problem, which can connect the problem with a singular initial term and the problem with a singular source term. That is in the following.

4.1. Duhamel's principle.

LEMMA 4.1 (Duhamel's principle). *The solution of the problem (1.3) is*

$$(4.1) \quad u(x, t) = \int_0^t v^s(x, t) ds,$$

where $v^s(x, t)$ is the solution of the problem

$$(4.2) \quad \begin{cases} v_t(x, t) + v_x(x, t) = 0, & (x, t) \in \Omega \times (s, \infty), \\ v(x, s) = \delta(x), & x \in \Omega. \end{cases}$$

Clearly, v^s is the solution to (4.2), where the initial condition at time $t = s$ is the source term of problem (1.3). We can simply check that u in (4.1) satisfies (1.3) to prove Lemma 4.1. See [23] for more details on the proof. Moreover, we can also prove that it is applicable for the approximation of two problems. Next, we give the semidiscrete version of Duhamel's principle.

Letting u_h be the approximation of the problem (1.3), it satisfies

$$(4.3) \quad \begin{cases} (\partial_t u_h, \chi)_{K_j(t)} = H_j(u_h, \chi) + (\delta, \chi)_{K_j(t)} \quad \forall \chi \in V_h(t), \\ u_h(0) = 0. \end{cases}$$

So, we have the following expression of u_h .

LEMMA 4.2. Define

$$(4.4) \quad u_h(x, t) = \int_0^t v_h^s(x, t) ds,$$

where v_h^s is the approximation of the problem (1.2), that is, it is the solution to

$$(4.5) \quad \begin{cases} (\partial_t v_h, \chi)_{K_j(t)} = H_j(v_h, \chi) \quad \forall \chi \in V_h(t), \\ v_h(s) = P_k(\delta(x)). \end{cases}$$

We can directly verify that u_h in (4.4) satisfies (4.3) directly from the independence between $K_j(t)$ and s and $(P_k(\delta(x)), \chi) = (\delta(x), \chi)$. That is, the lemma holds.

Next, we get the L^2 norm and several negative norm error estimates for problem (1.3) similar to (1.2) mainly using (4.1), (4.4), and the lemmas in section 3.3.

4.2. Error estimates.

THEOREM 4.3. Suppose u is the exact solution of (1.3), and u_h is the ALE-DG approximation which satisfies (4.3). Denote $R_T = (0 - C_* \log(1/h)h^{1/2}, T + C_* \log(1/h)h^{1/2})$, Then we have the following estimates:

$$(4.6) \quad \|u(T) - u_h(T)\|_{\Omega_1} \leq Ch^{k+1},$$

$$(4.7) \quad \|u(T) - u_h(T)\|_{-(k+1)} \leq Ch^k,$$

$$(4.8) \quad \|u(T) - u_h(T)\|_{-(k+2)} \leq Ch^{k+\frac{1}{2}},$$

$$(4.9) \quad \|u(T) - u_h(T)\|_{-(k+1), \Omega_1} \leq Ch^{2k+1},$$

where $\Omega_1 \subseteq \Omega \setminus R_T$. Here the mesh can be any one of the moving meshes.

Proof. We first prove (4.6) from (4.1), (4.4), and Theorem 3.5.

$$\begin{aligned} \|u(T) - u_h(T)\|_{\Omega_1} &= \left\| \int_0^T (v^s(x, T) - v_h^s(x, T)) ds \right\|_{\Omega_1} \\ &\leq \left\| \left(\int_0^T (v^s(x, T) - v_h^s(x, T))^2 ds \right)^{\frac{1}{2}} T^{\frac{1}{2}} \right\|_{\Omega_1} \\ &= T^{\frac{1}{2}} \left(\int_{\Omega_1} \int_0^T (v^s(x, T) - v_h^s(x, T))^2 ds dx \right)^{\frac{1}{2}} \\ &= T^{\frac{1}{2}} \left(\int_0^T \int_{\Omega_1} (v^s(x, T) - v_h^s(x, T))^2 dx ds \right)^{\frac{1}{2}} \\ &\leq T^{\frac{1}{2}} \left(\int_0^T (Ch^{k+1})^2 ds \right)^{\frac{1}{2}} \\ &\leq CT h^{k+1}. \end{aligned}$$

Next, we only prove (4.9), since the proofs of (4.7) and (4.8) are similar.

From (4.1), (4.4), and Theorem 3.13, we have

$$\begin{aligned}
\|u(T) - u_h(T)\|_{-(k+1), \Omega_1} &= \sup_{\Phi \in C_0^\infty(\Omega_1)} \frac{(u(T) - u_h(T), \Phi(x))}{\|\Phi\|_{k+1}} \\
&= \sup_{\Phi \in C_0^\infty(\Omega_1)} \frac{\left(\int_0^T (v^s - v_h^s)(T) ds, \Phi(x) \right)}{\|\Phi\|_{k+1}} \\
&= \sup_{\Phi \in C_0^\infty(\Omega_1)} \frac{\int_0^T ((v^s - v_h^s)(T), \Phi(x)) ds}{\|\Phi\|_{k+1}} \\
&\leq \sup_{\Phi \in C_0^\infty(\Omega_1)} \frac{\int_0^T \| (v^s - v_h^s)(T) \|_{-(k+1), \Omega_1} \|\Phi(x)\|_{k+1} ds}{\|\Phi\|_{k+1}} \\
&\leq \int_0^T \| (v^s - v_h^s)(T) \|_{-(k+1), \Omega_1} ds \\
&\leq \int_0^T Ch^{(2k+1)} ds \\
&\leq CT h^{(2k+1)}. \tag*{\square}
\end{aligned}$$

Therefore, Theorem 4.3 is proved. That is, we can also have similar error estimates for the case with a singular source term corresponding to the singular initial problem.

Remark 4.4. On static meshes, Yang and Shu in [34] gave the same error estimates with the smaller pollution region R_T as $I_i \cup (T - C_* h^{\frac{1}{2}} \log(1/h), T + C_* h^{\frac{1}{2}} \log(1/h))$. But it is not easy to apply the technique on the case over moving meshes, and thus we expand R_T into a larger pollution region in Theorem 4.3. In Example 3, numerically we can still observe that R_T stays bounded on moving meshes as on static meshes.

5. Adaptive moving meshes for δ -singularities. In this section, we discuss the generation of adaptive moving meshes for problem (1.1) involving δ -singularities. That is, we want put more points in the neighborhood of discontinuity to get mesh redistribution. We mainly follow Huang and co-authors [22, 21] and Tang and co-authors [31, 26]. We first denote the reference domain by $[0, 1]$ and the physical domain as Ω . The mesh transformation from the reference domain to the physical domain

$$x : \xi \mapsto x, [0, 1] \mapsto \Omega$$

can be obtained by the equidistribution principle

$$(5.1) \quad \frac{d(\rho(x) \frac{dx}{d\xi})}{d\xi} = 0,$$

where $\rho(x)$ is the given positive function, depend on the solution, the so-called mesh density function. We discretize (5.1) with central difference and Gauss-Seidel iteration:

$$(5.2) \quad \rho(u_{j+1}^{[n]})(x_{j+\frac{3}{2}}^{[n]} - x_{j+\frac{1}{2}}^{[n+1]}) - \rho(u_j^{[n]})(x_{j+\frac{1}{2}}^{[n+1]} - x_{j-\frac{1}{2}}^{[n+1]}) = 0,$$

where we denote the value of u in the $K_j(t_n)$ by $u_{j+1}^{[n]}$. Clearly, the mesh depends on the mesh density function ρ . The mesh density function is based on the error

indicator η_j . Here we adopt an indicator with arbitrary higher order derivative for smooth solutions by extending the indicator with first derivative designed by Li and Tang in [26]

$$(5.3) \quad \begin{aligned} \eta_j^{[n]} &= \sum_{l=0}^k ([\partial_x^{(l)} u_h(x_{j+\frac{1}{2}}, t)]^2 + [\partial_x^{(l)} u_h(x_{j-\frac{1}{2}}, t)]^2) h_{j+1}^{-(2*(k-l)+2)}, \\ \bar{\eta} &= \frac{1}{N} \sum_{j=1}^N \eta_j^{[n]}, \\ \rho(u_j^{[n]}) &= \sqrt{\bar{\eta} + \beta \min(\bar{\eta}, \eta_j^{[n]})}, \end{aligned}$$

where β is a mesh quality parameter. We may also choose different indicators according to different situations. Specifically, we choose

$$\eta_j^{[n]} = \left(\int_{x_{j-\frac{1}{2}}}^{x_{j+\frac{1}{2}}} u_h dx / h_j \right)^2$$

as the indicator and taking $\beta = 3$ in the last example, in which both the initial solution and equations do not contain the δ -singularities, but the δ -singularities gradually emerge in the exact solution with time evolving.

After we get the initial adaptive mesh, to improve the efficiency we adopt the moving mesh partial differential equation method [21], in which the mesh evolves as follows:

$$(5.4) \quad \frac{\partial x}{\partial t} = \frac{1}{\tau} \frac{\partial}{\partial \xi} \left(\rho \frac{\partial x}{\partial \xi} \right) = 0,$$

where the mesh density function is the same as above. For simplicity, we choose the relaxation time parameter $\tau = 1$.

According to this procedure, we can get the meshes which cluster more grid points to area with singularities. It is noteworthy that we still need a low-pass filter to improve the mesh smoothness and strict mesh movement restriction to keep stability. The restriction is to adjust repeatedly the adaptive mesh by reducing the time step to meet the CFL limit, which follows Huang and Russell in [22].

6. Numerical experiments. The aims of this section are applying the ALE-DG method and postprocessing technique on moving meshes to verify the theoretical analysis. For the following numerical examples, the initial discretization is obtained by taking the L^2 projection. And we apply the ALE-DG method with the local Lax–Friedrich flux to the spatial discretization by using P^k polynomials on moving meshes, and divide the domain into N intervals. We also adopt the seventh order Runge–Kutta time discretization (see [18]) and take the time step $\Delta t = \frac{0.1h}{\alpha(2k+1)}$, where $\alpha = \max(f'(u) - w)$ and $h = \min_{1 \leq j \leq N} h_j(t)$. In addition, we choose the local mesh size as the postprocessing scaling, $H = h_j$ according to [29], which performs better than the general fixed scaling.

Example 1. Singular initial condition problem.

We consider the following problem:

$$(6.1) \quad \begin{cases} u_t + u_x = 0, & x \in [0, \pi], \\ u(x, 0) = \delta(x - 0.5) + \sin(2x), & x \in [0, \pi], \end{cases}$$

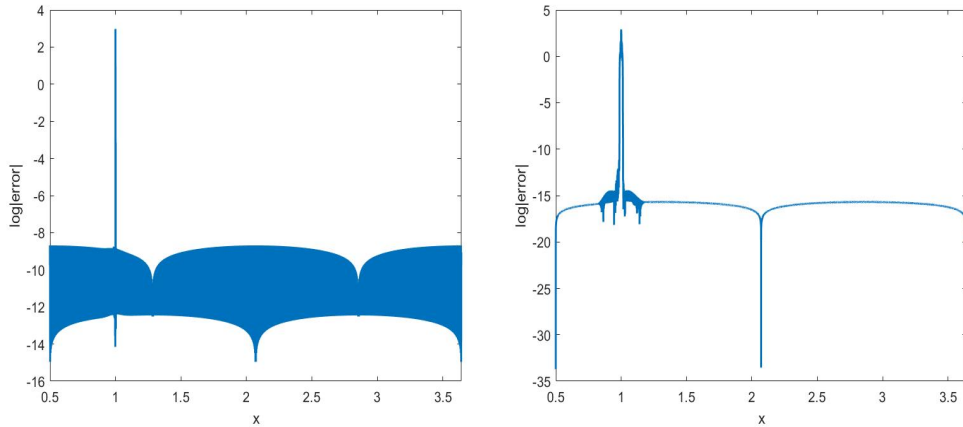


FIG. 1. Example 1: The errors of the ALE-DG solution without (left) and with (right) postprocessing on the moving mesh for $N = 1000$ and $k = 2$ at $T = 0.5$.

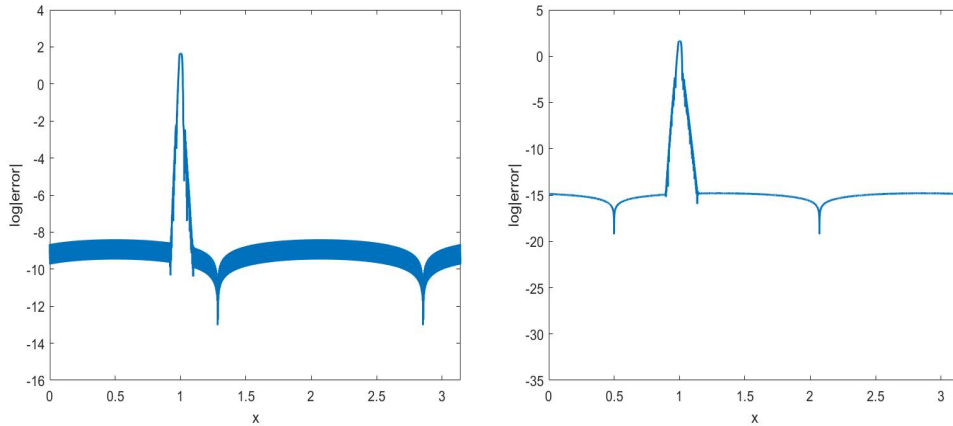


FIG. 2. Example 1: The errors of the ALE-DG solution without (left) and with (right) postprocessing on the uniform mesh for $N = 1000$, $k = 2$ at $T = 0.5$.

with periodic boundary condition. The exact solution for time $t < 1$ is

$$(6.2) \quad u(x, t) = \delta(x - t - 0.5) + \sin(2x - 2t).$$

We test this example on the uniform mesh and the moving mesh. The moving mesh is defined with an initial adaptive mesh and the grid velocity $w = 1$. We plot the errors of the ALE-DG solutions without/with postprocessing at time $T = 0.5$ in Figures 1 and 2 on the moving mesh and the uniform mesh, respectively. It shows that the pollution area on the moving mesh is much smaller than that on the uniform mesh, due to the mesh refinement near the singularity. Besides, the ALE-DG solutions on the moving mesh do not sacrifice the accuracy away from the pollution area, which is comparable to the results on the uniform mesh with the same mesh size N . We also show the L^2 and L^∞ -norm errors for the P^1 , P^2 , and P^3 ALE-DG solutions without/with the postprocessing in Table 1 and 2, respectively. From the tables, it verifies the $(k + 1)$ th order of accuracy for the ALE-DG solutions and the $(2k + 1)$ th

TABLE 1

Example 1: The L^2 and L^∞ -norm errors of the ALE-DG solutions in $[0, 0.8] \cup [1.2, \pi]$ on the uniform mesh, and $[0.5, 0.8] \cup [1.2, \pi + 0.5]$ on the moving mesh at $T = 0.5$.

| | N | Uniform mesh | | | | Moving mesh | | | |
|-------|------|--------------|-------|-------------------|-------|--------------|-------|-------------------|-------|
| | | L^2 -error | Order | L^∞ -error | Order | L^2 -error | Order | L^∞ -error | Order |
| P^1 | 400 | 2.04E-05 | - | 4.11E-05 | - | 1.10E-05 | - | 2.09E-05 | - |
| | 500 | 1.31E-05 | 2.00 | 2.63E-05 | 2.00 | 7.03E-06 | 2.00 | 1.32E-05 | 2.06 |
| | 600 | 9.06E-06 | 2.01 | 1.83E-05 | 2.00 | 4.88E-06 | 2.00 | 9.14E-06 | 2.01 |
| | 700 | 6.66E-06 | 2.00 | 1.34E-05 | 2.00 | 3.58E-06 | 2.00 | 6.71E-06 | 2.00 |
| | 800 | 5.10E-06 | 2.00 | 1.03E-05 | 2.00 | 2.74E-06 | 2.00 | 5.14E-06 | 2.00 |
| P^2 | 900 | 2.65E-09 | - | 5.67E-09 | - | 1.45E-09 | - | 2.84E-09 | - |
| | 1000 | 1.93E-09 | 3.00 | 4.13E-09 | 3.00 | 1.06E-09 | 3.00 | 2.07E-09 | 3.00 |
| | 1100 | 1.45E-09 | 3.00 | 3.11E-09 | 3.00 | 7.96E-10 | 3.00 | 1.55E-09 | 3.00 |
| | 1200 | 1.12E-09 | 3.00 | 2.39E-09 | 3.00 | 6.13E-10 | 3.01 | 1.20E-09 | 3.00 |
| | 1300 | 8.78E-10 | 3.00 | 1.88E-09 | 3.00 | 4.82E-10 | 2.99 | 9.41E-10 | 3.00 |
| P^3 | 900 | 1.20E-12 | - | 2.83E-12 | - | 6.67E-13 | - | 1.41E-12 | - |
| | 1000 | 7.86E-13 | 4.00 | 1.86E-12 | 4.00 | 4.37E-13 | 4.00 | 9.28E-13 | 4.00 |
| | 1100 | 5.36E-13 | 4.00 | 1.27E-12 | 4.00 | 3.00E-13 | 4.00 | 6.34E-13 | 4.00 |
| | 1200 | 3.79E-13 | 4.00 | 8.95E-13 | 4.00 | 2.11E-13 | 4.00 | 4.47E-13 | 4.00 |
| | 1300 | 2.75E-13 | 4.00 | 6.50E-13 | 4.00 | 1.53E-13 | 4.00 | 3.25E-13 | 4.00 |

TABLE 2

Example 1: The L^2 and L^∞ -norm errors of the postprocessed ALE-DG solutions in $[0, 0.8] \cup [1.2, \pi]$ on the uniform mesh, and $[0.5, 0.8] \cup [1.2, \pi + 0.5]$ on the moving mesh at $T = 0.5$.

| | N | Uniform mesh | | | | Moving mesh | | | |
|-------|------|--------------|-------|-------------------|-------|--------------|-------|-------------------|-------|
| | | L^2 -error | Order | L^∞ -error | Order | L^2 -error | Order | L^∞ -error | Order |
| P^1 | 400 | 8.96E-08 | - | 1.28E-06 | - | 1.05E-09 | - | 4.08E-09 | - |
| | 500 | 3.16E-08 | 4.67 | 3.26E-08 | 16.44 | 3.90E-10 | 4.46 | 1.48E-09 | 4.55 |
| | 600 | 1.83E-08 | 3.00 | 1.62E-08 | 3.84 | 1.76E-10 | 4.37 | 5.36E-10 | 5.57 |
| | 700 | 1.15E-08 | 3.01 | 1.01E-08 | 3.04 | 9.28E-11 | 4.14 | 1.81E-10 | 7.04 |
| | 800 | 7.70E-09 | 3.01 | 6.77E-09 | 3.01 | 5.43E-11 | 4.02 | 7.42E-11 | 6.68 |
| P^2 | 900 | 3.06E-15 | - | 4.50E-15 | - | 4.41E-16 | - | 4.04E-16 | - |
| | 1000 | 1.78E-15 | 5.14 | 2.62E-15 | 5.14 | 2.34E-16 | 6.00 | 2.08E-16 | 6.31 |
| | 1100 | 1.09E-15 | 5.13 | 1.61E-15 | 5.13 | 1.32E-16 | 6.00 | 1.17E-16 | 6.05 |
| | 1200 | 7.00E-16 | 5.12 | 1.03E-15 | 5.12 | 7.85E-17 | 6.00 | 6.92E-17 | 6.00 |
| | 1300 | 4.65E-16 | 5.11 | 6.84E-16 | 5.11 | 4.86E-17 | 6.00 | 4.28E-17 | 6.00 |
| P^3 | 900 | 7.44E-21 | - | 6.53E-21 | - | 6.79E-21 | - | 6.55E-21 | - |
| | 1000 | 3.23E-21 | 7.91 | 2.84E-21 | 7.91 | 2.92E-21 | 8.00 | 2.68E-21 | 8.47 |
| | 1100 | 1.52E-21 | 7.90 | 1.34E-21 | 7.90 | 1.36E-21 | 8.00 | 1.21E-21 | 8.34 |
| | 1200 | 7.66E-22 | 7.89 | 6.73E-22 | 7.89 | 6.79E-22 | 8.00 | 5.97E-22 | 8.15 |
| | 1300 | 4.08E-22 | 7.88 | 3.58E-22 | 7.88 | 3.58E-22 | 8.00 | 3.14E-22 | 8.00 |

convergence rate for the postprocessed ALE-DG solutions in the smooth area both on the uniform and moving meshes. For the same mesh size N , the error of the ALE-DG solution on the moving mesh is slightly smaller than that on the uniform mesh due to the smaller pollution area.

Example 2. Singular initial condition system.

For simplicity, we only state the theory for scalar linear equations in the previous sections, but it is also applicable to linear systems. We consider the following linear system with the singular initial condition,

$$(6.3) \quad \begin{cases} u_t - v_x = 0, & x \in [0, 2], \\ v_t - u_x = 0, & x \in [0, 2], \\ u(x, 0) = \delta(x - 1), v(x, 0) = 0, & x \in [0, 2], \end{cases}$$

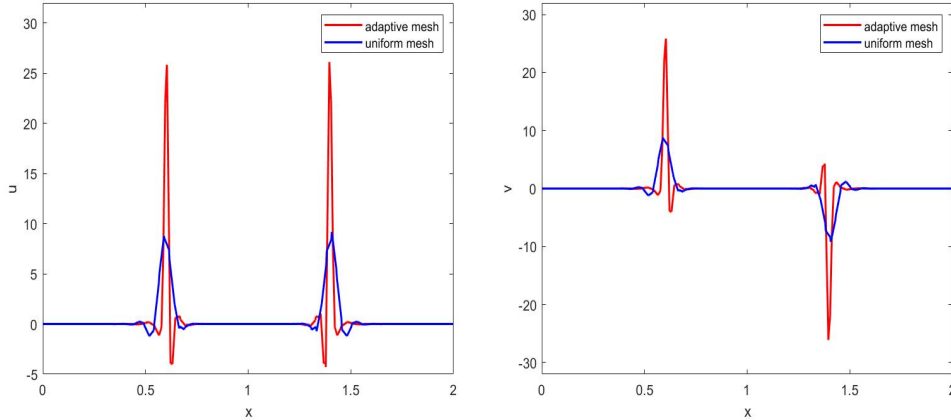


FIG. 3. Example 2: The ALE-DG solutions u (left) and v (right) with $N = 81$, P^1 polynomial at $T = 0.4$ on the uniform mesh and adaptive moving mesh, respectively.

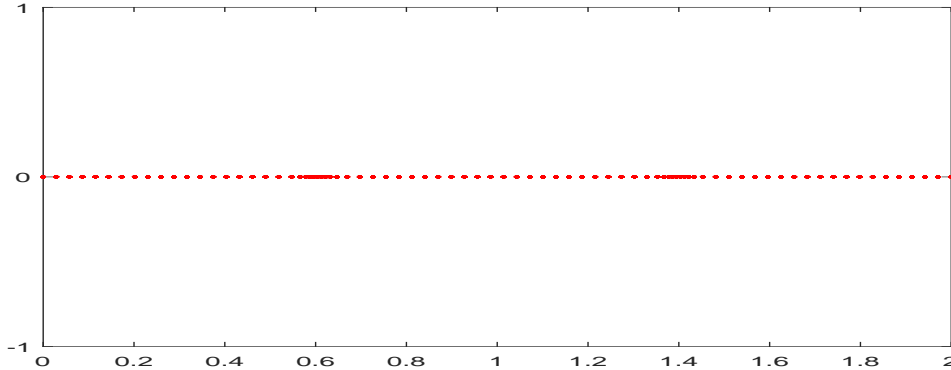


FIG. 4. Example 2: The adaptive moving mesh with $N = 81$, P^1 polynomial at $T = 0.4$.

and the periodic boundary condition. Using Green's function, we get the exact solution as follows:

$$\begin{aligned} u(x, t) &= \frac{1}{2}\delta(x - 1 + t) + \frac{1}{2}\delta(x - 1 - t), \\ v(x, t) &= \frac{1}{2}\delta(x - 1 + t) - \frac{1}{2}\delta(x - 1 - t). \end{aligned}$$

We plot the ALE-DG solutions at $T = 0.4$ for P^1 polynomials with $N = 81$ on the uniform mesh and adaptive moving mesh in Figure 3. The adaptive moving mesh is obtained according to the algorithm in section 5. We can clearly see that the ALE-DG solution on the adaptive moving mesh captures the singularities more sharply than the solution on the uniform mesh. In Figure 4, we also plot the adaptive moving mesh at $T = 0.4$. It shows that the mesh points concentrate near the singularities, which leads to the better performance of the ALE-DG method on the adaptive moving mesh than on the uniform mesh.

TABLE 3

Example 3: The L^2 and L^∞ -norm errors of the ALE-DG solutions with P^2 polynomials without (left) and with (right) postprocessing in $[0, 2.5] \cup [4.5, 2\pi]$ on the moving meshes.

| N | Without postprocessing | | | | After postprocessing | | | |
|------|------------------------|-------|-------------------|-------|----------------------|-------|-------------------|-------|
| | L^2 -error | Order | L^∞ -error | Order | L^2 -error | Order | L^∞ -error | Order |
| 801 | 4.07E-09 | - | 8.04E-09 | - | 4.20E-15 | - | 2.82E-15 | - |
| 901 | 2.86E-09 | 3.00 | 5.65E-09 | 3.00 | 2.29E-15 | 5.16 | 1.53E-15 | 5.22 |
| 1001 | 2.09E-09 | 3.00 | 4.12E-09 | 3.00 | 1.33E-15 | 5.12 | 8.81E-16 | 5.22 |
| 1101 | 1.57E-09 | 3.00 | 3.10E-09 | 3.00 | 8.21E-16 | 5.10 | 5.36E-16 | 5.21 |
| 1201 | 1.21E-09 | 3.00 | 2.39E-09 | 3.00 | 5.27E-16 | 5.09 | 3.41E-16 | 5.21 |

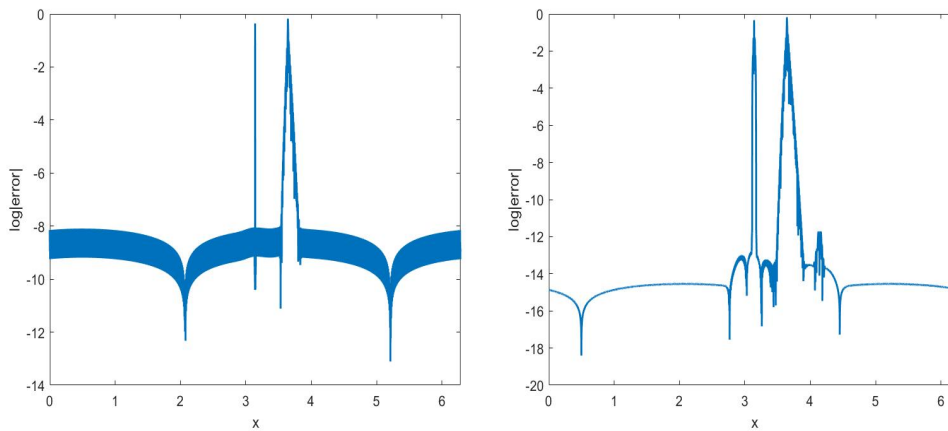


FIG. 5. Example 3: The errors without (left) and with (right) postprocessing on the moving mesh with $N = 801$, P^2 polynomial.

Example 3. Singular source term problem.

Next, we solve the following singular source term problem:

$$(6.4) \quad \begin{cases} u_t + u_x = \delta(x - \pi), & x \in [0, 2\pi], \\ u(x, 0) = \sin(x), & x \in [0, 2\pi], \end{cases}$$

with the periodic boundary condition. The exact solution is

$$(6.5) \quad u(x, t) = \sin(x - t) + \chi_{[\pi, \pi+t]},$$

where $\chi_{[a, b]}$ denotes the indicator function of the interval $[a, b]$. We test the ALE-DG scheme with P^2 polynomials. The moving mesh is chosen by connecting the initial adaptive mesh with the final adaptive mesh at $T = 0.5$. In Table 3, we present the L^2 and L^∞ errors without/with postprocessing in the smooth region $[0, 2.5] \cup [4.5, 2\pi]$ at time $T = 0.5$. We can observe the optimal convergence rate in accordance with the theoretical analysis. The errors without/with the postprocessing are plotted in Figure 5. It shows that the postprocessing technique is effective in the smooth region.

Example 4. Rendezvous algorithm.

The final example is devoted to the following nonlinear problem,

$$(6.6) \quad \begin{cases} \rho_t + F_x = 0, & x \in [0, 1], t > 0, \\ \rho(0, x) = 1, & \end{cases}$$

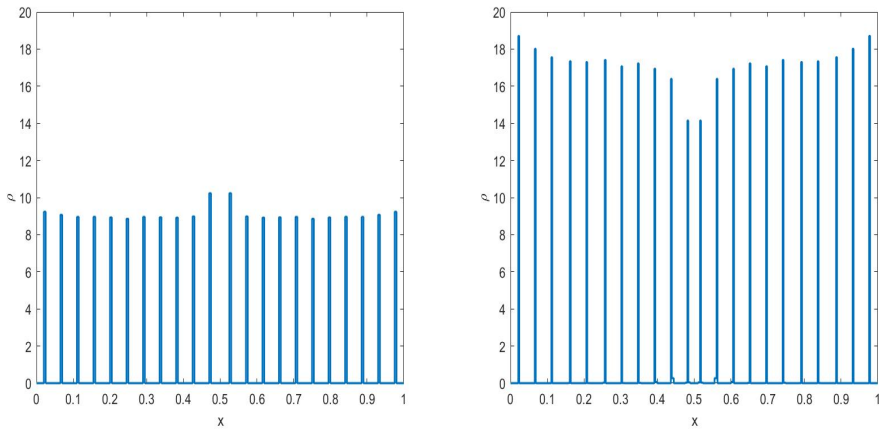


FIG. 6. Example 4: The ALE-DG solutions at $T = 1000$ on the uniform mesh (left) and adaptive moving mesh (right) with $N = 200$, P^0 polynomial.

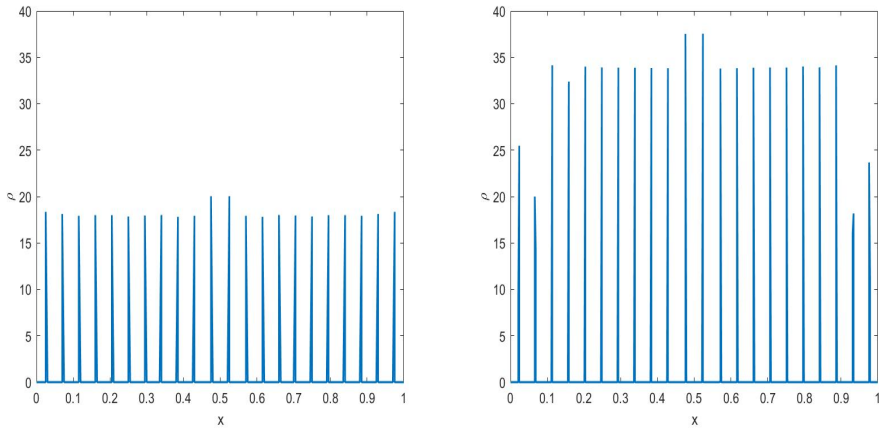


FIG. 7. Example 4: The ALE-DG solutions at $T = 1000$ on the uniform mesh (left) and adaptive moving mesh (right) with $N = 200$, P^1 polynomial.

where ρ is always a positive function and F is defined by $F(t, x) = v(t, x)\rho(t, x)$. The v is given that $v(t, x) = \int(y - x)\xi(y - x)\rho(t, y)dy$, where $\xi(x) = \chi[-R, R]$. Canuto, Fagnani, and Tilli investigated the PDE and its discretized version in [2] and proved that the solution ρ will converge to some singularities when t tends to infinity. In addition, they also found that the number of those singularities is dependent on R and the distances between those singularities must be greater than R . Here we choose $R = 0.02$. We use the ALE-DG scheme and the third order strong stability preserving (SSP) Runge–Kutta time discretization in [16] with $\Delta t = 0.1h$. Note that the positive-preserving limiter in [37] is needed when using P^1 polynomials. In Figures 6 and 7, we plot the ALE-DG solutions at $T = 1000$ with P^0 and P^1 polynomials on the uniform mesh and adaptive moving mesh with $N = 200$, respectively. The adaptive moving mesh is generated by the algorithm in section 5 with the indicator

$$\eta_j^{[n]} = \left(\int_{x_{j-\frac{1}{2}}}^{x_{j+\frac{1}{2}}} u_h dx / h_j \right)^2$$

and $\beta = 3$. In all cases, we can observe 22 singularities as the result in [2, 34]. But the height of δ -singularities is almost doubled on the adaptive moving meshes compared to the uniform meshes, which leads to less smearing of δ -singularities due to the conservative property of the scheme. A similar situation can be observed when comparing with the P^0 solutions and P^1 solutions.

7. Concluding remarks. In this paper, we presented and analyzed the ALE-DG method to solve hyperbolic conservation laws involving δ -singularities on moving meshes. We investigated the accuracy including L^2 -norm and the negative norm error estimates of the ALE-DG approximations to linear hyperbolic equations with singular initial condition or singular source terms. Numerically we demonstrated the stability and the optimal convergence rates of ALE-DG solutions in accordance with the theoretical analysis. The results also show that the ALE-DG method has better performance on adaptive moving meshes than static meshes.

REFERENCES

- [1] J. H. BRAMBLE AND A. H. SCHATZ, *Higher order local accuracy by averaging in the finite element method*, Math. Comp., 31 (1977), pp. 94–111.
- [2] C. CANUTO, F. FAGNANI, AND P. TILLI, *An Eulerian approach to the analysis of Rendez-vous algorithms*, IFAC Proc. Vol., 41 (2008), pp. 9039–9044.
- [3] P. CIARLET, *The Finite Element Method for Elliptic Problem*, North-Holland, Amsterdam, 1975.
- [4] B. COCKBURN AND J. GUZMÁN, *Error estimate for the Runge–Kutta discontinuous Galerkin method for transport equation with discontinuous initial data*, SIAM J. Numer. Anal., 46 (2008), pp. 1364–1398.
- [5] B. COCKBURN, S. HOU, AND C.-W. SHU, *The Runge–Kutta local projection discontinuous Galerkin finite element method for conservation laws IV: The multidimensional case*, Math. Comp., 54 (1990), pp. 545–581.
- [6] B. COCKBURN, G. E. KARNIADAKIS, AND C.-W. SHU, *Discontinuous Galerkin Methods—Theory, Computation and Applications*, Lect. Notes Comput. Sci. Eng. 11, Springer, New York, 2000.
- [7] B. COCKBURN, S. Y. LIN, AND C.-W. SHU, *TVB Runge–Kutta local projection discontinuous Galerkin finite element method for conservation laws III: One-dimensional systems*, J. Comput. Phys., 84 (1989), pp. 90–113.
- [8] B. COCKBURN, M. LUSKIN, C.-W. SHU, AND E. SÜLI, *Enhanced accuracy by post-processing for finite element methods for hyperbolic equations*, Math. Comp., 72 (2003), pp. 577–606.
- [9] B. COCKBURN AND C.-W. SHU, *TVB Runge–Kutta local projection discontinuous Galerkin finite element method for conservation laws II: General framework*, Math. Comp., 52 (1989), pp. 411–435.
- [10] B. COCKBURN AND C.-W. SHU, *The Runge–Kutta discontinuous Galerkin method for conservation laws V: Multidimensional systems*, J. Comput. Phys., 141 (1998), pp. 199–224.
- [11] B. COCKBURN AND C.-W. SHU, *The local discontinuous Galerkin method for time-dependent convection–diffusion systems*, SIAM J. Numer. Anal., 35 (1998), pp. 2440–2463.
- [12] B. COCKBURN AND C.-W. SHU, *Runge–Kutta discontinuous Galerkin methods for convection-dominated problems*, J. Sci. Comput., 16 (2001), pp. 173–261.
- [13] Y. N. DI, R. LI, T. TANG, AND P. W. ZHANG, *Moving mesh finite element methods for the incompressible Navier–Stokes equations*, SIAM J. Sci. Comput., 26 (2005), pp. 1036–1056.
- [14] J. DONEA, A. HUERTA, J. P. PONTHOT, AND A. RODRÍGUEZ-FERRAN, *Arbitrary Lagrangian–Eulerian Methods*, Part 1. Fundamentals, in Encyclopedia of Computational Mechanics, E. Stein, R. De Borst, and T. J. R. Hughes, eds., Wiley, New York, 1, 2004, pp. 413–437.
- [15] P. FU, G. SCHNUCKE, AND Y. XIA, *Arbitrary Lagrangian–Eulerian discontinuous Galerkin method for conservation laws on moving simplex meshes*, Math. Comp., 88 (2019), pp. 2221–2255.
- [16] S. GOTTLIEB, C.-W. SHU, AND E. TADMOR, *Strong stability-preserving high-order time discretization methods*, SIAM Rev., 43 (2001), pp. 89–112.
- [17] H. GUILLARD AND C. FARHAT, *On the significance of the geometric conservation law for flow computations on moving meshes*, Comput. Methods Appl. Mech. Engrg., 190 (2000), pp. 1467–1482.

- [18] E. HAIER, G. WANNER, AND S. P. NORSETT, *Solving Ordinary Differential Equations I: Nonstiff Problems*, Springer Ser. Comput. Math. 8, Springer, New York, 1987.
- [19] J. S. HESTHAVEN AND T. WARBURTON, *Nodal Discontinuous Galerkin Methods, Algorithms, Analysis, and Applications*, Springer, New York, 2008.
- [20] C. W. HIRT, A. A. AMSDEN, AND J. L. COOK, *An arbitrary Lagrangian-Eulerian computing method for all flow speeds*, J. Comput. Phys., 14 (1974), pp. 227–253.
- [21] W. Z. HUANG, Y. REN, AND R. D. RUSSELL, *Moving mesh partial differential equations (MMPDEs) based upon the equidistribution principle*, SIAM J. Numer. Anal., 31 (1994), pp. 709–730.
- [22] W. Z. HUANG AND R. D. RUSSELL, *Adaptive Moving Mesh Methods*, Appl. Math. Sci. 174, Springer, New York, 2010.
- [23] F. JOHN, *Partial differential equations*, Springer, New York (1971).
- [24] C. KLINGENBERG, G. SCHNÜCKE, AND Y. XIA, *Arbitrary Lagrangian-Eulerian discontinuous Galerkin method for conservation laws: Analysis and application in one dimension*, Math. Comput., 86 (2017), pp. 1203–1232.
- [25] C. KLINGENBERG, G. SCHNÜCKE, AND Y. XIA, *An arbitrary Lagrangian-Eulerian local discontinuous Galerkin method for Hamilton-Jacobi equations*, J. Sci. Comput., 73 (2017), pp. 906–942.
- [26] R. LI AND T. TANG, *Moving mesh discontinuous Galerkin method for hyperbolic conservation laws*, J. Sci. Comput., 27 (2006), pp. 347–363.
- [27] X. LI, J. K. RYAN, R. M. KIRBY, AND C. VUIK, *Smoothness-increasing accuracy-conserving (SIAC) filters for derivative approximations of discontinuous Galerkin (DG) solutions over nonuniform meshes and near boundaries*, J. Comput. Appl. Math., 294 (2016), pp. 275–296.
- [28] W. H. REED AND T. R. HILL, *Triangular Mesh Methods for the Neutron Transport Equation*, Los Alamos Scientific Laboratory report LA-UR-73-479, Los Alamos, NM, 1973.
- [29] J. RYAN, X. LI, R. M. KIRBY, AND C. VUIK, *One-sided position-dependent smoothness-increasing accuracy-conserving (SIAC) filtering over uniform and non-uniform meshes*, J. Sci. Comput., 64 (2015), pp. 773–817.
- [30] C.-W. SHU, *Discontinuous Galerkin methods: General approach and stability*, in Numerical Solutions of Partial Differential Equations, S. Bertoluzza, S. Falletta, G. Russo, and C.-W. Shu, eds., Adv. Courses Math. CRM Barcelona, Birkhäuser, Basel, Switzerland, 2009, pp. 149–201.
- [31] H. Z. TANG AND T. TANG, *Adaptive mesh methods for one- and two-dimensional hyperbolic conservation laws*, SIAM J. Numer. Anal., 41 (2003), pp. 487–515.
- [32] Q. TAO AND Y. XU, *Superconvergence of arbitrary Lagrangian-Eulerian discontinuous Galerkin methods for linear hyperbolic equations*, SIAM J. Numer. Anal., 57 (2019), pp. 2142–2165.
- [33] Y. XU AND C.-W. SHU, *Local discontinuous Galerkin methods for high-order time-dependent partial differential equations*, Commun. Comput. Phys., 7 (2010), pp. 1–46.
- [34] Y. YANG AND C.-W. SHU, *Discontinuous Galerkin method for hyperbolic equations involving δ -singularities: Negative-order norm error estimates and applications*, Numer. Math., 124 (2013), pp. 753–781.
- [35] Q. ZHANG AND C.-W. SHU, *Error estimates to smooth solutions of Runge-Kutta discontinuous Galerkin methods for scalar conservation laws*, SIAM J. Numer. Anal., 42 (2004), pp. 641–666.
- [36] Q. ZHANG AND C.-W. SHU, *Error estimates for the third order explicit Runge-Kutta discontinuous Galerkin method for linear hyperbolic equation in one-dimension with discontinuous initial data*, Numer. Math., 126 (2014), pp. 703–740.
- [37] X. ZHANG AND C.-W. SHU, *On positivity preserving high order discontinuous Galerkin schemes for compressible Euler equations on rectangular meshes*, J. Comput. Phys., 229 (2010), pp. 8918–8934.
- [38] L. ZHOU, Y. XIA, AND C.-W. SHU, *Stability analysis and error estimates of arbitrary Lagrangian-Eulerian discontinuous Galerkin method coupled with Runge-Kutta time-marching for linear conservation laws*, ESAIM Math. Model. Numer. Anal., 53 (2019), pp. 105–144.